NASA TECHNICAL NOTE

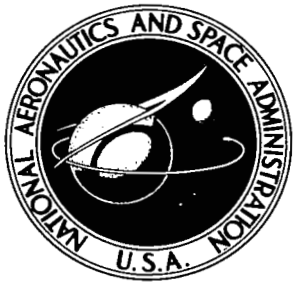

NASA TN D-7028

VALIDATION OF THE GAS GENERATOR METHOD OF CALCULATING JET-ENGINE THRUST AND EVALUATION OF XB-70-1 AIRPLANE ENGINE PERFORMANCE AT GROUND STATIC CONDITIONS

by Henry H. Arnaiz and William G. Schweikhard

Flight Research Center
Edwards, Calif. 93523

NATIONAL AERONAUTICS AND SPACE ADMINISTRATION • WASHINGTON, D. C. • DECEMBER 1970

1. Report No.	2. Government Accession No.	3. Recipient's Catalog No.
NASA TN D-7028		

4. Title and Subtitle	5. Report Date
VALIDATION OF THE GAS GENERATOR METHOD OF CALCULATING JET-ENGINE THRUST AND EVALUATION OF XB-70-1 AIRPLANE ENGINE PERFORMANCE AT GROUND STATIC CONDITIONS	December 1970
	6. Performing Organization Code

7. Author(s)	8. Performing Organization Report No.
Henry H. Arnaiz and William G. Schweikhard	H-596
	10. Work Unit No.
	720-51-00-07-24

9. Performing Organization Name and Address	11. Contract or Grant No.
NASA Flight Research Center P. O. Box 273 Edwards, California 93523	
	13. Type of Report and Period Covered
12. Sponsoring Agency Name and Address	Technical Note
National Aeronautics and Space Administration Washington, D. C. 20546	14. Sponsoring Agency Code

15. Supplementary Notes

16. Abstract

Deficiencies in established techniques of measuring aircraft thrust in flight led to the application of the gas generator method of calculating engine thrust to the XB-70-1 airplane. A series of tests on a ground static-thrust stand was performed on the airplane to establish at ground static conditions the accuracy of this method, to measure the installed thrust of the YJ93-GE-3 engine, and to determine the effect of instrumentation errors and nonuniform flows at the engine compressor face on the thrust calculation. Tests with an aerodynamically choked inlet, an opened inlet-bypass system, and varying combinations of operating engines were also conducted.

Results showed that the accuracy of the gas generator method was ±2 percent for the normal operation of the XB-70-1 airplane at ground static conditions and for the upper 70 percent of the engine's throttle range. They also showed that the effect of individual instrument errors on the thrust calculation was reduced because of the large number of measurements and that abnormally high inlet flow distortion affects the thrust calculation.

When corrected for inlet losses, the installed thrust of the YJ93-GE-3 engine agreed favorably with the engine manufacturer's uninstalled estimated thrust for all power settings except those at the low end.

17. Key Words (Suggested by Author(s))	18. Distribution Statement
XB-70-1 airplane - In-flight thrust - Thrust measurement	Unclassified - Unlimited

19. Security Classif. (of this report)	20. Security Classif. (of this page)	21. No. of Pages	22. Price*
Unclassified	Unclassified	43	$3.00

*For sale by the National Technical Information Service, Springfield, Virginia 22151

VALIDATION OF THE GAS GENERATOR METHOD OF CALCULATING JET-ENGINE THRUST AND EVALUATION OF XB-70-1 AIRPLANE ENGINE PERFORMANCE AT GROUND STATIC CONDITIONS

Henry H. Arnaiz and William G. Schweikhard
Flight Research Center

INTRODUCTION

Evaluating an aircraft's performance and verifying wind-tunnel drag predictions in flight is highly dependent on an accurate measurement of engine net thrust. Because this measurement is difficult to obtain in flight for high-performance aircraft powered by turbojets, many procedures and techniques, depending on the aircraft, engines, and test conditions, have been tried.

Most procedures for determining the in-flight net thrust of turbojet aircraft can be categorized into three methods: (1) a method that uses engine gas-flow data (temperatures and pressures) obtained at the engine exit plane by a traversing-rake apparatus (refs. 1 and 2); (2) a commonly used method that, with an indication of engine power setting (for example, rpm), utilizes test-cell or thrust-stand data extrapolated to flight Mach numbers and altitude by corrected or normalized engine-cycle parameters $\left(\frac{F_n}{\delta}, \frac{N}{\sqrt{\theta}}, \frac{W\sqrt{\theta}}{\delta}\right)$; and (3) a method that, by using a nozzle coefficient, combines exhaust nozzle gas probe measurements with test-cell or thrust-stand data (refs. 3 and 4). Unfortunately, most methods, except in very limited instances, have not produced data with the accuracy needed for flight testing (within 5 percent), so that improvement of these techniques or the development of a new and better method is needed.

Recently, a procedure called the "gas generator method" (refs. 1 and 5) was used to calculate in-flight engine net thrust for the XB-70-1 airplane during the aircraft's flight-test program. Preliminary performance calculations suggested that a high degree of accuracy in the thrust calculation could be achieved throughout the airplane's Mach number and altitude range (Mach numbers of 0 to 3 and altitudes of 0 to 80,000 feet (24,400 meters)). In order to further investigate the accuracy of this method for validation and in-flight thrust determinations, it was decided to conduct a series of ground static-thrust-stand tests.

The series of static-thrust-stand tests of the XB-70-1 airplane was performed at the Edwards Air Force Base static-thrust calibration facility. The tests were designed to: (1) determine a level of accuracy for the thrust-calculating procedure at ground static conditions; (2) investigate the sensitivity of the thrust-calculating procedure to instrumentation errors and normal and abnormal inlet and engine operating conditions; (3) determine the static thrust of the YJ93-GE-3 engine installed in the

airplane; (4) investigate the effects on the airplane's propulsion system of high inlet flow distortion levels, inlet choking, and use of the XB-70-1 inlet bypass system as an auxiliary inlet, and (5) evaluate the noise generated by the XB-70-1 engines as a function of engine power, inlet setting, and distance between operating engines.

This report presents the results from these tests that are related to the XB-70-1 engine performance and the evaluation of the thrust-calculating procedure. In addition, the basic calculating procedure of the gas generator method is described briefly.

SYMBOLS

The units for the physical quantities defined in this report are given both in U.S. Customary Units and in the International System of Units (SI). (See ref. 6.)

A	engine nozzle area, inches^2 (meters^2)
A_c	inlet capture area, inches^2 (meters^2)
$\frac{A_d}{A_a}$	ratio of an area of below-average pressure to the annulus area of the engine compressor face
A_e	effective nozzle area, inches^2 (meters^2)
A_t	inlet throat area, inches^2 (meters^2)
D	engine-face distortion, $\frac{p_{t,2_{max}} - p_{t,2_{min}}}{p_{t,2_{av}}} 100$, percent
$E_{(\ )}$	error in net thrust between method indicated by subscript and $F_{n,meas}$, $\frac{F_{n,(\ )} - F_{n,meas}}{F_{n,meas}} 100$, percent
F_g	gross thrust, pounds (newtons)
F_n	net thrust, pounds (newtons)
$F_{n,(\ )}$	net thrust obtained by the method indicated by subscript, pounds (newtons)
$F_{n,k}$	corrected net thrust as defined by equations (1) and (2), pounds (newtons)
F_r	ram drag, pounds (newtons)
M	Mach number

N	engine rotor speed, rpm
p	static pressure, pounds/inches^2 (newtons/meters^2)
p_t	total pressure, pounds/inches^2 (newtons/meters^2)
T_t	total temperature, degrees Rankine or degrees Fahrenheit (degrees Kelvin or degrees Celsius)
W	engine airflow, pounds/second (kilograms/second)
$W_{f,AB}$	afterburner fuel flow, pounds/second (kilograms/second)
$W_{f,m}$	main engine fuel flow, pounds/second (kilograms/second)
$W_{f,t}$	total engine fuel flow, pounds/second (kilograms/second)
W_{S7}	engine secondary airflow, pounds/second (kilograms/second)
δ	ratio of total pressure to standard-day sea-level pressure, $\frac{p_t}{p_{sl}}$
θ	ratio of total temperature to standard-day sea-level temperature, $\frac{T_t}{T_{sl}}$

Subscripts:

A_8	A_8 alternate path method of calculating net thrust
av	average value
calc	weight-flow-path method of calculating net thrust
max	maximum value
meas	thrust measured by thrust stand
min	minimum value
p_7	p_7 alternate path method of calculating net thrust
sl	standard sea-level conditions
∞	free-stream or ambient conditions

Engine station numbers (fig. 1):

2	compressor inlet
3	compressor discharge

4	turbine inlet
5	turbine discharge
6	afterburner inlet
7	primary nozzle inlet
S7	jet-nozzle secondary air inlet
8	primary nozzle exit
9	secondary nozzle exit

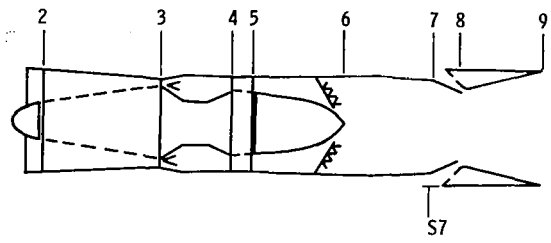

Figure 1. Location of engine stations on the YJ93-GE-3 engine.

AIRPLANE AND PROPULSION SYSTEM

The XB-70 airplane (fig. 2) was designed as a weapons system with long-range, supersonic-cruise capabilities. The airplane had a design gross weight in excess of 500,000 pounds (227,000 kilograms) and a design cruising speed of Mach 3.0 at altitudes of 70,000 to 80,000 feet (21,300 to 24,400 meters).

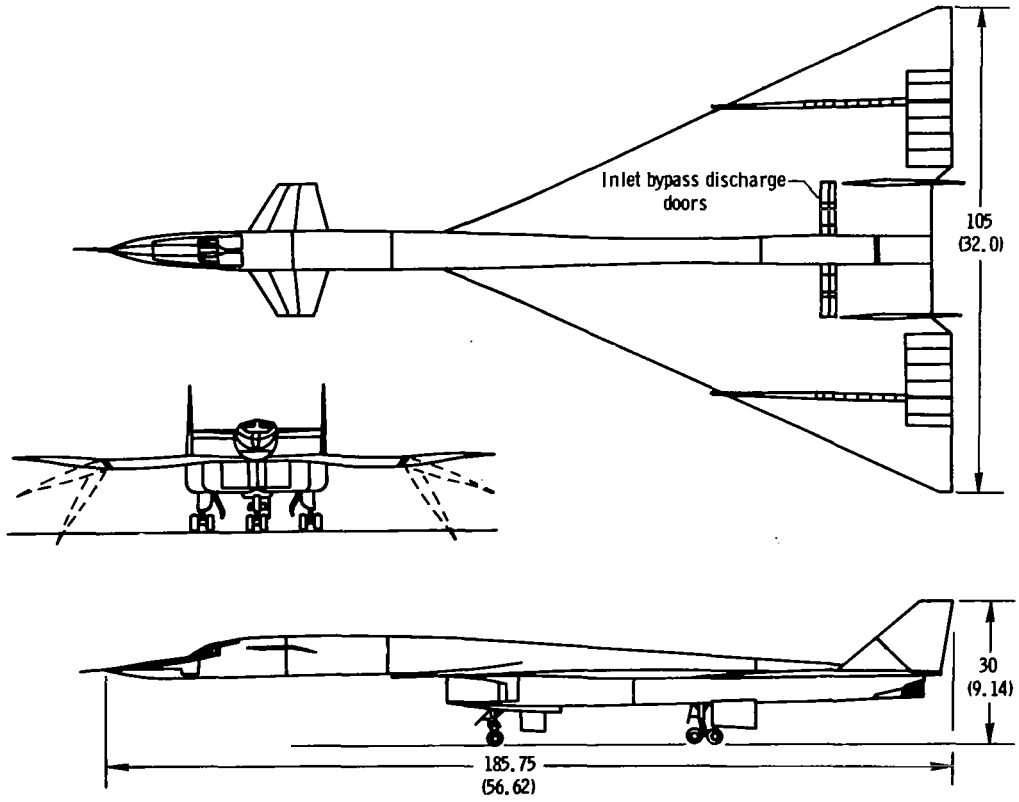

Figure 2. Three-view drawing of the XB-70-1 airplane. Dimensions in feet (meters).

Propulsion was provided by six YJ93-GE-3 engines (fig. 3). Each engine had a 30,000-pound (133,400-newton) sea-level static-thrust classification with a compressor airflow capability of 264 pounds (120 kilograms) per second and an 8.7 to 1 pressure ratio. Each engine was equipped with an 11-stage axial-flow compressor with variable stators, an annular combustion system, a two-stage air-cooled turbine, and a variable-area, convergent-divergent exhaust nozzle with secondary airflow.

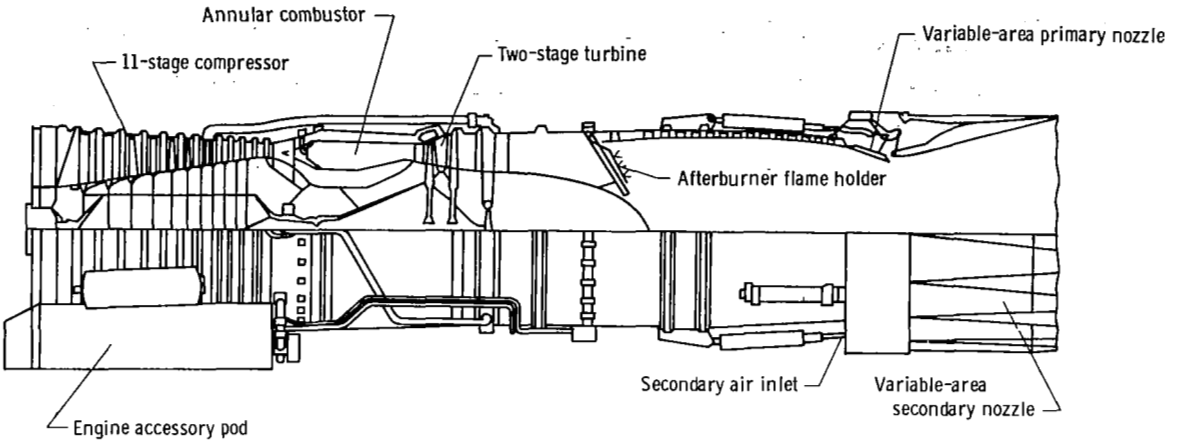

(a) Cutaway view of the YJ93-GE-3 engine.

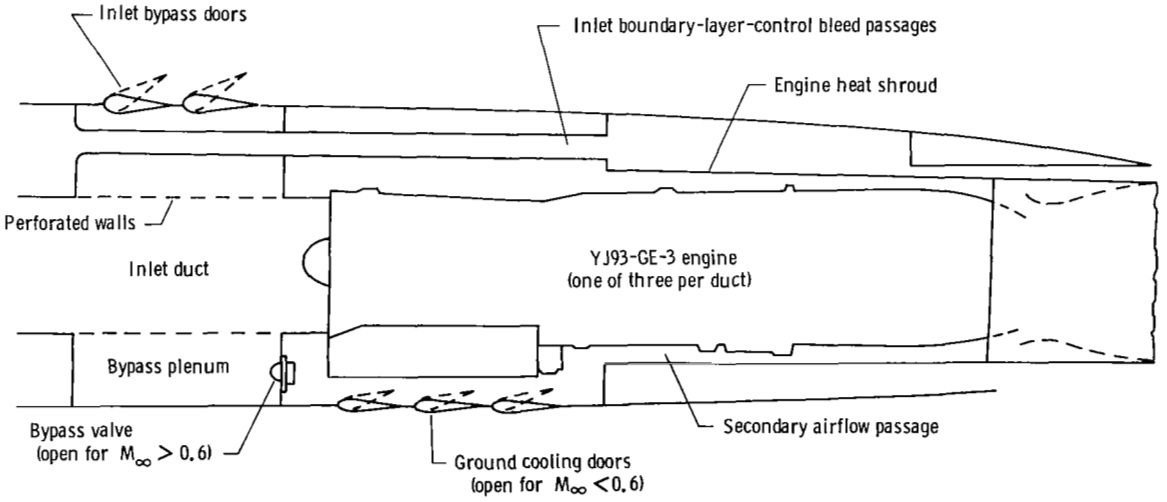

(b) YJ93-GE-3 engine in the installed position.

Figure 3. Schematic drawing of the XB-70-1 engine and installation.

The six engines were mounted side by side in the rear of the fuselage in a single nacelle under the center section of the wing (figs. 2 and 4). The nacelle was divided

into twin, two-dimensional, vertical-ramp, mixed-compression inlets incorporating variable ramp positions and throat areas for optimum operation throughout the Mach number range.

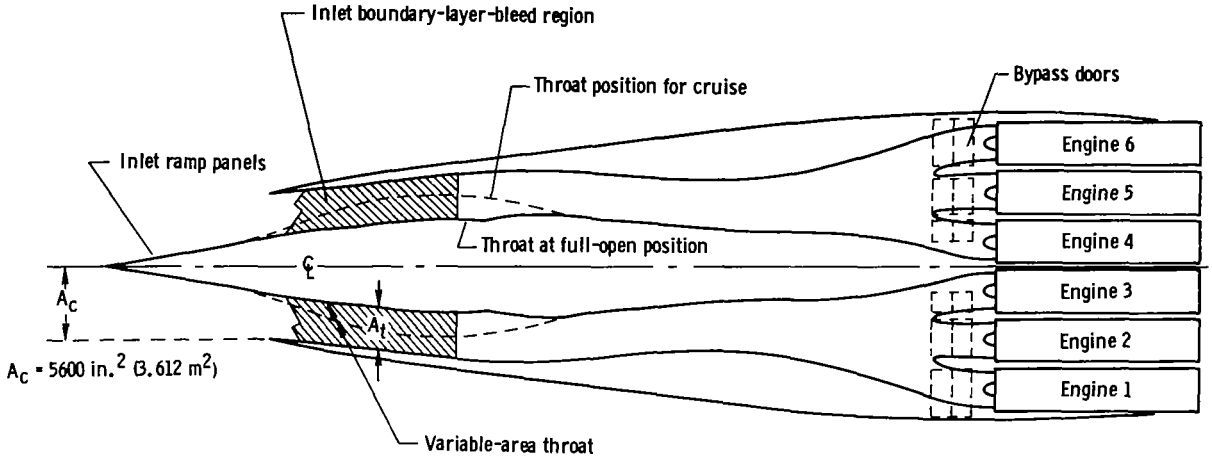

Figure 4. Schematic drawing of the XB-70-1 airplane variable-throat inlet and engine configuration. Top view.

The left- and right-hand air-intake ducts were equipped with inlet-air bypass doors on top of each duct just forward and inboard of the leading edge of the vertical fins (figs. 2, 3(b), and 4). These doors were used in conjunction with the variable two-dimensional throats to control the position of the normal shock in each of the ducts and to match engine airflow requirements.

The XB-70 incorporated inlet boundary-layer-air extraction. Boundary-layer air was bled through perforated panels (fig. 4) at the ramp region of the air-inlet ducts. Part of the bleed air was dumped overboard just behind and below the inlet opening, and the rest was distributed to the base region of the aircraft. (See fig. 3.)

General physical characteristics of the airplane are included in reference 7 and more detailed characteristics, in reference 8.

INSTRUMENTATION AND TEST FACILITIES

The data from the XB-70-1 ground static-thrust tests were gathered from a number of sources; however, the bulk of the information was obtained from the XB-70-1 data-acquisition system and the static-thrust calibration facility.

XB-70-1 Data-Acquisition System

The XB-70-1 airplane was instrumented for flight testing with approximately 800 to 900 recording data sensors installed throughout the vehicle. Sensor signals were transmitted to a specially designed airborne data package, housed in the weapons bay of the airplane, where signal conditioning, sampling, telemetering, digitizing, and

recording of the data signal took place. Data, recorded on magnetic tape by the airborne data package, were reduced by a ground base data-reduction facility. The data package and the reduction facility are discussed in detail in references 9 to 11.

A detailed description of the aircraft instrumentation used for these tests is presented in appendix A. These instruments and their accuracies, ranges, and sampling rates are listed in table 1.

TABLE 1. XB-70-1 INSTRUMENTATION FOR THE GROUND STATIC-THRUST TEST

(a) Pressures.

Description	Accuracy, percent full range	Sensor range,		Type of pressure	Sample rate per sec
		lb/in^2	N/m^2		
Nose-boom total pressure	0.05	0 to 30	0 to 20,700	Absolute	20
Free-stream static pressure	.05	0 to 20	0 to 13,800	Absolute	20
Reference pressure 1	.05	0 to 15	0 to 10,300	Absolute	20
Reference pressure 2	.05	0 to 30	0 to 20,700	Absolute	20
Reference pressure 3	.05	0 to 20	0 to 13,800	Absolute	20
Left-hand-inlet unstart-signal static pressure	.66	±15	±10,300	Differential	40
Left-hand-inlet throat-region static pressure, 7 sensors	2.5	±6	±4100	Differential	40
Left-hand-inlet throat-region static pressure, 3 sensors	2.5	±15	±10,300	Differential	40
Zone 1 left-hand boundary-layer-control bleed-chamber forward static pressure	2.5	±6	±4100	Differential	20
Zone 1 left-hand boundary-layer-control bleed-chamber exit static pressure	2.0	±4	±2800	Differential	4
Zone 1 left-hand boundary-layer-control bleed-chamber exit total pressure	2.0	±6	±4100	Differential	4
Zone 2 left-hand boundary-layer-control bleed-chamber forward static pressure	2.5	±10	±6900	Differential	20
Zone 2 left-hand boundary-layer-control bleed-chamber exit static pressure	2.0	±6	±4100	Differential	20
Zone 2 left-hand boundary-layer-control bleed-chamber exit total pressure	2.0	±6	±4100	Differential	4
Zone 3 left-hand boundary-layer-control bleed-chamber forward static pressure	2.0	±6	±4100	Differential	20
Zone 3 left-hand boundary-layer-control bleed-duct exit static pressure	2.0	±6	±4100	Differential	4
Zone 4A left-hand boundary-layer-control bleed-chamber forward static pressure	2.0	±10	±6900	Differential	20
Zone 4B left-hand boundary-layer-control bleed-chamber forward static pressure	2.0	±10	±6900	Differential	20
Zone 5 left-hand boundary-layer-control bleed-chamber static pressure	2.0	±10	±6900	Differential	20
Secondary-air static pressure at engine compressor region, engines 1, 2, 3	2.0	±2	±1400	Differential	4
Secondary-air static pressure at engine primary exhaust-nozzle region (p_{S7}), engines 2, 3	2.0	±6	±4100	Differential	4
Engine compressor-face-rake total pressure ($p_{t,2}$), 5 probes per rake, 4 rakes per engine, engines 1, 2, 3, 4	1.5	±6	±4100	Differential	4
Engine compressor-face-rake static pressure (p_2), 1 probe per rake, 4 rakes per engine, engines 1, 2, 3, 4	1.5	±6	±4100	Differential	4
Engine compressor-face-hub total pressure ($p_{t,2}$) engines 1, 2, 3, 4, 5, 6	1.5	±6	±4100	Differential	4
Engine compressor-discharge static pressure (p_3), engines 1, 2, 3, 4, 5, 6	2.0	±20	±13,800	Differential	100
Engine turbine-discharge total pressure ($p_{t,5}$), low range, 2 rakes per engine, engines 1, 2, 3, 4, 5, 6	2.0	±6	±4100	Differential	4
Engine turbine-discharge total pressure ($p_{t,5}$), high range, 2 rakes per engine, engines 1, 2, 3, 4, 5, 6	2.0	±40	±27,500	Differential	4
Engine tailpipe static pressure (p_7), low range, engines 1, 2, 3, 4, 5, 6	2.0	±6	±4100	Differential	4
Engine tailpipe static pressure (p_7), high range, engines 1, 2, 3, 4, 5, 6	2.0	±40	±27,500	Differential	4
Fuselage left-hand base-region static pressures, 11 sensors	2.0	±3	±2000	Differential	4

TABLE 1. Concluded.

(b) Temperatures.

Description	Accuracy, percent full range	Sensor range, deg F	Sensor range, deg C	Sample rate per sec
Free-stream-air total temperature, low range	1.2	-75 to 325	-60 to 160	20
Inlet-air total temperature at engine compressor face ($T_{t,2}$) engines 1, 3	1.2	-100 to 1650	-73 to 900	4
Secondary-air total temperature at primary exhaust-nozzle region ($T_{t,S7}$), engines 1, 3	1.2	-100 to 1650	-73 to 900	4
Main-engine-manifold fuel temperature, engines 1, 2, 3, 4, 5, 6	1.2	-100 to 1650	-73 to 900	4
Afterburner-fuel temperature, engines 1, 2, 3, 4, 5, 6	1.2	-100 to 1650	-73 to 900	4
Engine 3 total fuel temperature	1.2	-100 to 1650	-73 to 900	4
Engine turbine-discharge total temperature ($T_{t,5}$) engines 1, 2, 3, 4, 5, 6	1.2	650 to 2450	340 to 1340	4
Engine primary-nozzle "pucker string" temperature, engines 1, 2, 3, 4, 5, 6	1.2	-100 to 1650	-73 to 900	4

(c) Positions.

Description	Accuracy, percent full range	Range	Sample rate per sec
Bypass-door position on left-hand inlet, one-half travel, 6 doors	2.0	0 to 19	40
Bypass-door position on left-hand inlet, full travel, doors 1, 3, 5	1.2	0 to 38	40
Inlet-throat-ramp forward position, left- and right-hand inlet, 2 sensors	1.2	0 to 31 in. (0.79 m)	20
Inlet-throat-ramp aft position, left- and right-hand inlet, 2 sensors	1.2	0 to 31 in. (0.79 m)	20
Engine 3 forward-stator position	2.0	45 to 15	4
Engine 3 aft-stator position	2.0	15 to 40	4
Engine power-control-lever position, engines 1, 2, 3, 4, 5, 6	1.2	0° to 125°	4
Engine primary-nozzle position, engines 1, 2, 3, 4, 5, 6	2.0	25 in. (0.64 m) to 35 in. (0.9 m)	4
Engine secondary-nozzle position, engines 1, 2, 3, 4, 5, 6	2.0	0 to 36 in. (0.91 m)	4

(d) Miscellaneous.

Description	Accuracy, percent full range	Sensor range	Sample rate per sec
Shock position ratio	2.0	1.0 to 3.0	20
Engine rpm, engines 1, 2, 3, 4, 5, 6	1.0	0 to 7500 rpm	20
Engine total-fuel flow ($W_{f,t}$), engines 1, 2, 3, 4, 5, 6	1.0	0 to 60,000 lb hr (0 to 75.6 kg sec)	4
Engine main-fuel flow ($W_{f,m}$), engines 1, 2, 3, 4, 5, 6	1.3	10 to 87 gal min (0.038 to 0.329 m^3/min)	100
Engine afterburner-fuel flow ($W_{f,AB}$), engines 1, 2, 3, 4, 5, 6	2.0	10 to 130 gal/min (0.038 to 0.492 m^3 min)	100

Static-Thrust Calibration Facility

For the XB-70-1 ground static-thrust tests, the Edwards Air Force Base static-thrust calibration facility was used to measure the XB-70-1 thrust. The facility consists of four loading platforms (each capable of measuring up to 125,000 pounds (556,000 newtons) of thrust), a data-recording system, and test monitoring equipment. Of the three platforms used for this test, the XB-70-1 airplane was secured to only two (fig. 5).

The accuracy of the static-thrust calibration facility for these tests was ±300 pounds (±1330 newtons) for thrust values from 0 to 40,000 pounds (177,900 newtons) and ±600 pounds (±2669 newtons) for thrust values from 40,000 to 150,000 pounds (177,900 to 667,200 newtons). These accuracies were obtained from calibrations performed

before and after the static-thrust tests and are valid for the asymmetric load condition of platforms 1 and 2 (fig. 5). A more detailed description of this facility is presented in appendix B.

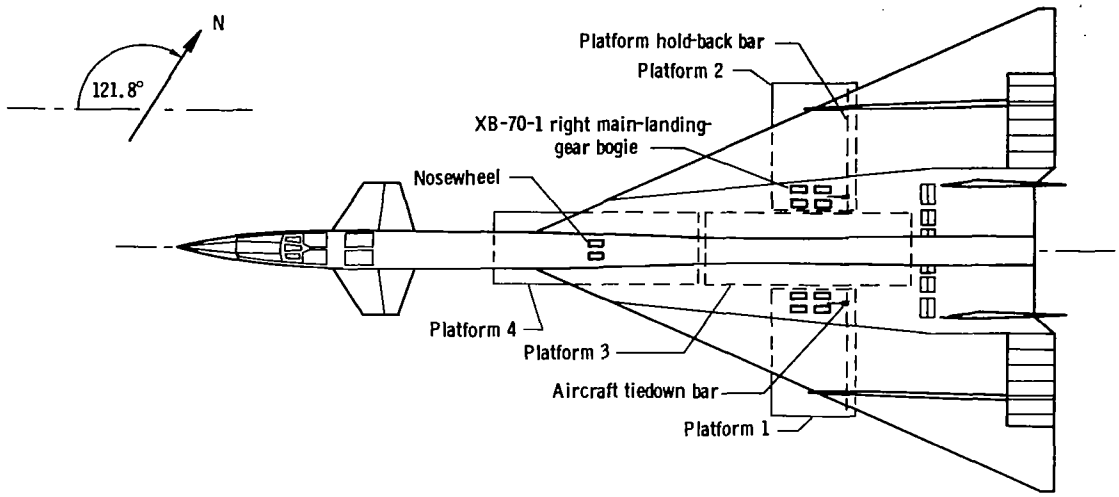

Figure 5. Schematic drawing of the XB-70-1 airplane in the static-thrust calibration facility. Top view.

GAS GENERATOR METHOD OF CALCULATING ENGINE NET THRUST

Description of the Gas Generator Method

The net thrust of a turbojet engine (difference between the gross thrust and the ram drag) can be determined if the weight flow, pressure, and temperature of the gases entering the engine inlet and leaving the nozzle exit are known. A direct and accurate measurement of the latter gas properties is usually limited by a high-temperature environment at the engine nozzle exit, especially for afterburning conditions.

A method has been developed by the manufacturer of the YJ93-GE-3 engine that determines the properties of the gases at the engine inlet and exit from indirect measurements and known engine operating characteristics. This method, the gas generator method (ref. 5), calculates gas-flow properties through the engine by combining a select group of aircraft and engine measurements with the operating characteristics of certain engine components (for example, compressor, combustor, jet nozzle). This method is based on the use of the conservation equations of mass and energy along with the known thermodynamic and fluid dynamic behavior of the engine components.

The characteristics of the engine components were obtained from extensive wind-tunnel and test-cell testing of several YJ93-GE-3 engines, engine components, and models of the components. The engine characteristics resulting from these tests represent what is considered to be the "average" YJ93-GE-3 engine and are used in the calculations.

An outline of the basic procedure used to calculate the engine net thrust by the gas generator method is shown in the block diagram of figure 6. This procedure, which has been simplified for clarity, is performed by a complex computer program that contains engine characteristic data, several iteration procedures, and a multitude of computer operations. The method is described briefly in the following paragraphs; further details are included in reference 5.

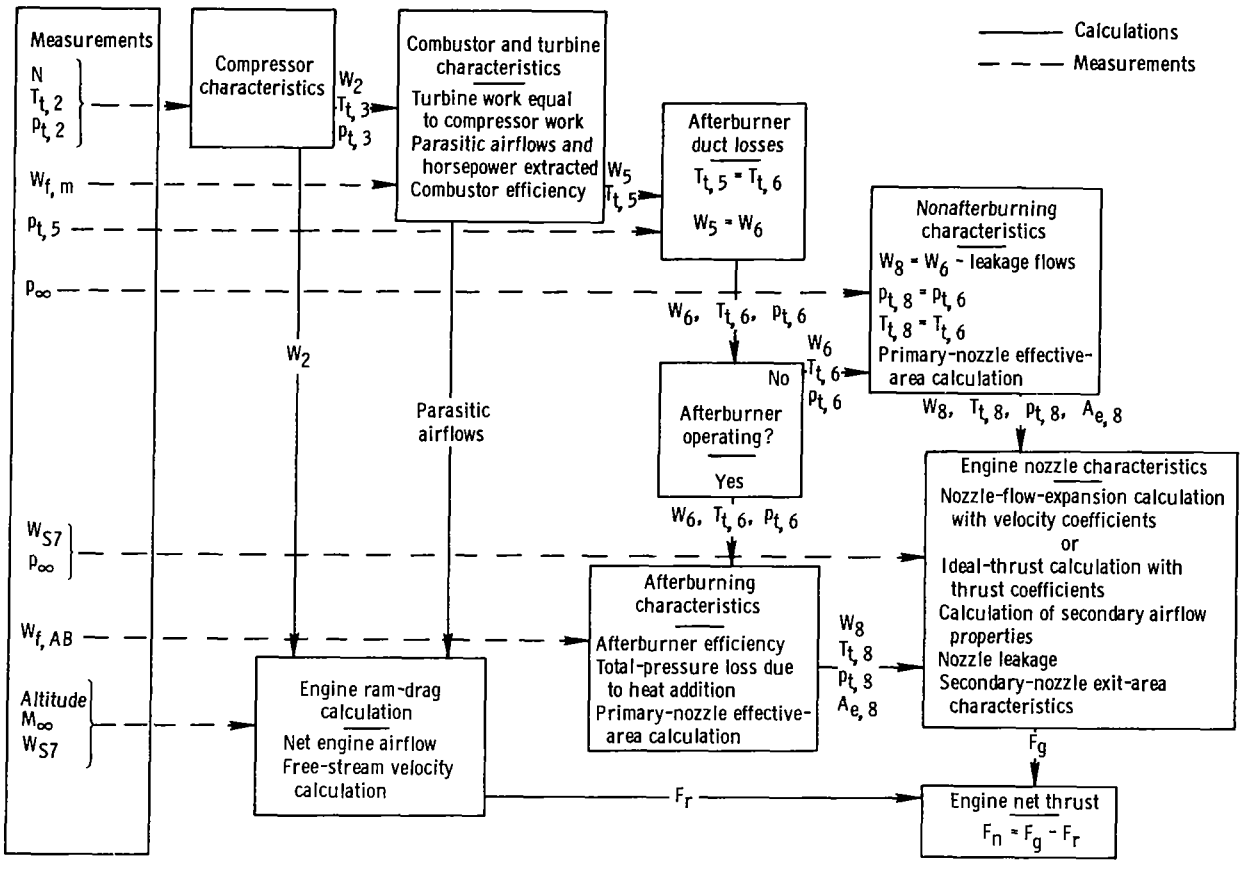

Figure 6. Block diagram of the procedure used in the gas generator method to calculate engine net thrust.

As shown in the upper left corner of figure 6, the program starts by combining the measured engine speed N, $p_{t,2}$, and $T_{t,2}$ with the compressor characteristics to obtain engine airflow W_2, $p_{t,3}$, and $T_{t,3}$. By assuming that turbine work is equal to the compressor work and using the combustor and turbine characteristics with W_2, $p_{t,3}$, $T_{t,3}$, and the measured main engine fuel flow ($W_{f,m}$), the turbine discharge gas flow W_5 and total temperature $T_{t,5}$ can be obtained. Horsepower extracted and parasitic airflow, which is the airflow that is extracted from the engine, are accounted for in this step. With the measured turbine discharge pressure $p_{t,5}$, W_5, and $T_{t,5}$, and the afterburner duct losses, which include the flame holder, turbine frame strut, innercone diffuser, and afterburner liner friction losses, $T_{t,6}$ and $p_{t,6}$ are obtained.

After determining if the afterburner is operating, the next step is to obtain the effective exit area of the primary nozzle $A_{e,8}$, total pressure $p_{t,8}$, total temperature $T_{t,8}$, and gas weight flow of both the primary and secondary streams W_8 and W_{S7}. For the afterburner operating, this step is performed by applying the afterburner characteristics and afterburner fuel-flow measurement. For the afterburner not operating, the total pressure and temperature are assumed to be constant through the engine tailpipe. Leakage flow through the primary nozzle and the primary nozzle effective area $A_{e,8}$ are calculated for choked nozzle flow at station 8. When the nozzle is not choked, p_∞ is also used in obtaining $A_{e,8}$.

After the parameter values at station 8 have been established, one of three procedures, depending on the ratios of $\frac{p_{t,8}}{p_\infty}$ and $\frac{A_9}{A_8}$, is used to calculate nozzle exit flow conditions.

For $\frac{p_{t,8}}{p_\infty}$ and $\frac{A_9}{A_8}$ such that the secondary nozzle flow is underexpanded, the primary and secondary streams are expanded independently to an identical static pressure at the nozzle exit in a manner that allows the combined exit areas of both streams to equal the exit area of the secondary nozzle A_9. By knowing the ambient static pressure, the exit area of the primary nozzle, and the gas flow properties of station 8, the ideal gross thrust can be determined. Actual engine gross thrust is obtained by multiplying the momentum term of the ideal gross thrust by a velocity coefficient which accounts for nonaxial flow, friction, and profile effects.

For $\frac{p_{t,8}}{p_\infty}$ and $\frac{A_9}{A_8}$ such that the secondary nozzle flow is overexpanded, the nozzle flow is isentropically expanded to the free-stream static pressure to produce an ideal thrust. The engine gross thrust is obtained by multiplying this ideal thrust by a nozzle thrust coefficient. For the XB-70-1 ground static-thrust tests, the gross thrust was obtained by this procedure.

For $\frac{p_{t,8}}{p_\infty}$ and $\frac{A_9}{A_8}$ such that the nozzle flow is correctly expanded at A_9, the calculation interpolates between the two preceding procedures.

In flight, the engine ram drag is determined from the net engine airflow and the aircraft free-stream velocity. Engine net thrust is then obtained by subtracting the ram drag from the engine gross thrust.

After the basic gas-flow properties through the engine have been established, other gas-flow properties at each engine station (fig. 1) can be obtained by using engine geometry and characteristics.

One feature that makes the gas generator method attractive for use in flight testing is that many of the engine parameters calculated by this procedure can be checked with a direct measurement (where measurements are possible) or a redundant calculation based on independently measured parameters. This feature allows both calculated and

measured parameters to be cross-checked so that instrumentation errors can be kept to a minimum. It also provides a backup measurement for most of the measured parameters needed in the thrust calculation. Some of the more important measured parameters used for redundancy checks are p_2, $T_{t,5}$, p_7, A_8, and A_9. The redundant calculations are engine primary airflow, engine secondary airflow, and engine thrust.

Redundant Thrust Calculations

Cross-checks of the engine net-thrust calculation are built into the program of the gas generator method, in that the engine net thrust is calculated by three methods, referred to as paths. The "weight-flow path," the primary calculation, utilizes the total heat input from the fuel flow and conservation-of-energy concepts to obtain the basic calculation of engine thrust. The second path, the "A_8 alternate path," utilizes the measured exit area A_8 of the primary nozzle and mass flow continuity. The third path, the "p_7 alternate path," is closely related to the weight-flow path except that the primary-nozzle total pressure $p_{t,8}$ is obtained from a calibration and the measurement of p_7 instead of $p_{t,5}$, with the assumption that the primary nozzle (station 8) is choked.

Although the three paths are not completely independent of each other, a good check of the key measured parameters can be obtained. The weight-flow-path calculation of engine net thrust, which is the primary engine thrust calculation, is considered to be the most accurate of the three. The thrust calculated by the weight-flow path is referred to in this report as the calculated thrust $F_{n,calc}$.

Analysis of the Thrust-Calculation Accuracy

The level of accuracy that can be obtained by the gas generator method of calculating engine thrust depends mainly on two factors: (1) how accurately the engine component characteristics (obtained from wind-tunnel and test-cell data, for an average engine) describe the operation of a specific installed engine at a given test condition, and (2) the accuracy (of the measuring instruments) with which engine parameters can be measured.

Numerical studies (examples are included in ref. 5) conducted to determine the effects of parameter-measurement errors on the engine thrust calculation indicate that the thrust-calculation procedure should be highly tolerant of small instrument errors. Figure 7 presents the results of this study for some of the key engine parameters of the weight-flow-path thrust calculation at the conditions experienced on the XB-70-1 ground static-thrust test (approximately 2300 ft (700 m) altitude and 0 Mach number). The figure shows that, with the exception of $p_{t,5}$ at low power-control-lever angles, a 1-percent incremental change in any one engine parameter resulted in much less than a 1-percent change in the calculated thrust of that engine.

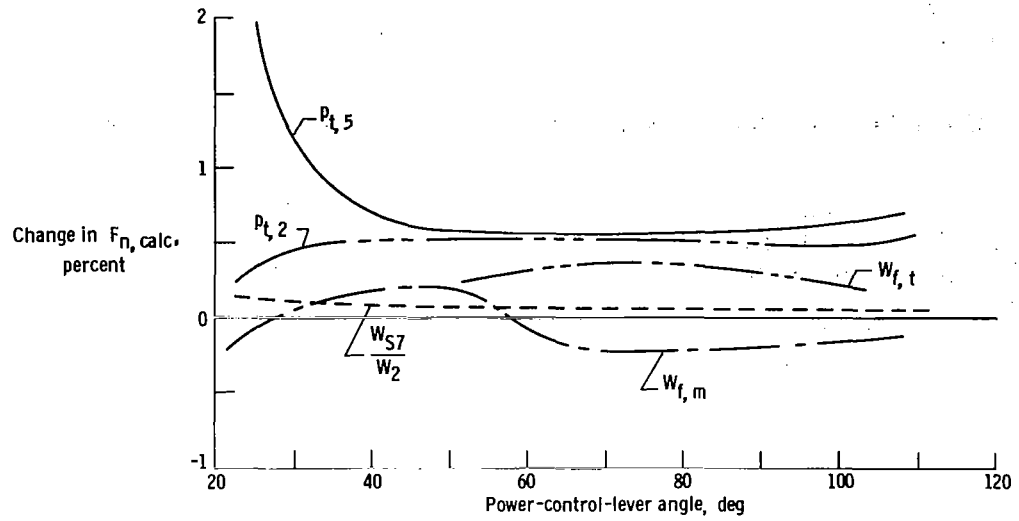

Figure 7. Percentage change in calculated net thrust as a function of power-control-lever angle for positive 1.0-percent errors in the parameters shown. M_∞ = 0; altitude = 2300 feet (700 meters).

Another reason for the tolerance for small instrument errors is that random errors or erroneous instrument readings are reduced by the following conditions: (1) All data samples (see the instrument sampling rate in table 1) taken over a 2-second interval for each measurement are averaged to reduce the dynamic or noise errors in the data. (2) Some of the input parameters are an average of several measurements (for example, $p_{t,2}$ is the average of 20 different total-pressure measurements taken at the engine compressor face). (3) Because of the many measurements and the measurement of the corresponding parameters on the six engines (for example, the $p_{t,5}$ measurement), the net effect on the total thrust from one error is significantly reduced by the correct measurement of other parameters or the compensating effect of another error of comparable magnitude that is opposite in sign.

It should be mentioned that before the computer program is to be used to calculate the engine thrust, input parameters which are obviously in error (because of faulty or inoperative instrumentation) must be replaced with approximate values. This procedure has been necessary because the computer program will not operate successfully unless certain parameters are within a nominal range for the normal operation of the engine. Other obvious deviations from nominal performance must be replaced to refine the final thrust calculation so that the error resulting from the deviation will not significantly affect the final results. The value of the replaced parameter is based on engineering judgment that is influenced by a combination of (1) a comparison of identical parameters on different engines operating near or at the same condition, (2) experience with the thrust data from numerous thrust calculations, (3) a comparison between measured and predicted values for certain parameters, and (4) a complete knowledge of the XB-70-1 thrust-calculating procedure. In some instances, errors may become apparent only after a thrust calculation has been performed, which sometimes requires additional calculations with corrected data.

For the thrust values calculated from the XB-70-1 ground static-thrust test data, the number of parameters replaced for any one calculation varied between 5 and 23.

DESCRIPTION OF THE XB-70-1 GROUND STATIC-THRUST TESTS

The XB-70-1 airplane was secured to the Edwards Air Force Base static-thrust calibration facility to undergo a series of static ground tests on four days in the latter part of 1967. (See figs. 5 and 8.) The tests required that engine runs be performed with different power settings, inlet conditions, and inlet flow distortions, and different combinations of operating engines (from one- to six-engine runs). These requirements were made by the following series of tests:

1. Inlet sweep runs (foreign object damage (FOD) screens installed)
2. Normal six-engine operation
3. Different combinations of operating engines
4. Inlet throat choking test
5. Inlet bypass test
6. Miscellaneous tests

Each test condition and the procedure used to perform each test are described in appendix C.

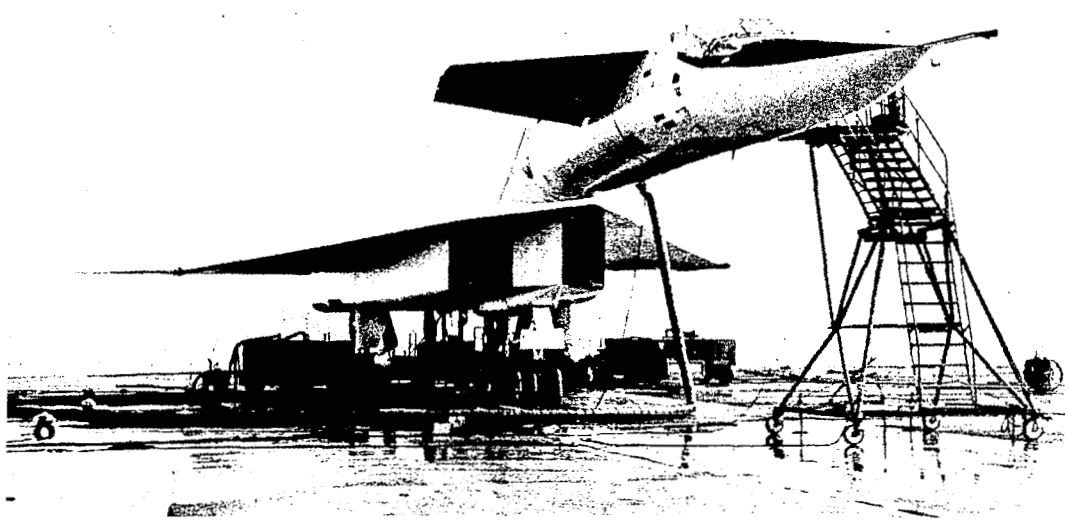

Figure 8. XB-70-1 airplane undergoing ground static testing in the static-thrust calibration facility.

A total of 193 test points was obtained. The engine power settings, left-hand inlet conditions, measured thrust values, and ambient conditions are presented for each run in appendix C (table 2). Engine power settings are shown as power-control-lever angle; these values can be converted to percent rpm for part-speed power points

by using the plot in figure 9. The measured thrust values and the wind velocity and direction were obtained from the static-thrust calibration facility. Other atmospheric conditions were obtained from the Edwards Air Force Base weather service. Variations in inlet configuration were used only for the left-hand inlet; the right-hand inlet configuration was constant throughout the test (throat full open, bypass doors closed).

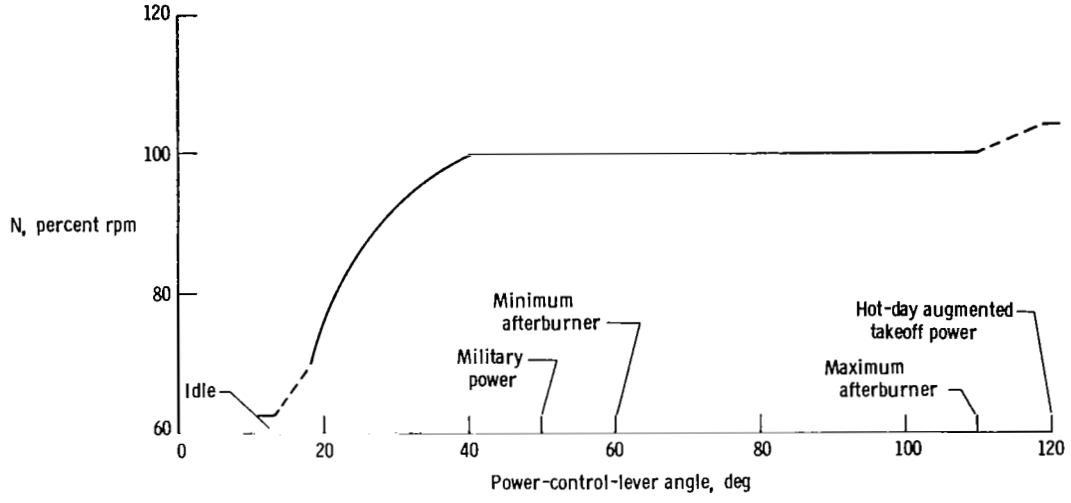

Figure 9. Relationship between engine power control and engine percent speed for the tests. 100 percent rpm = 6825 rpm.

For each test, the engines were allowed to stabilize at each test point for 1 minute when in an afterburner power setting and for 2 minutes for power settings that required a change in engine rpm. Data recorders were then turned on, and the data were recorded for 30 seconds. The test setup is described in appendix C.

RESULTS AND DISCUSSION

Comparison of Measured and Calculated Thrust

Thrust values for each test point were obtained from the three thrust-calculating paths of the gas generator method ($F_{n,calc}$, F_{n,p_7}, and F_{n,A_8}) and from the static-thrust calibration facility measurements $F_{n,meas}$. These values are compared and the comparison analyzed in the next two sections.

Results from the weight-flow-path calculation of thrust. – The percent error E_{calc} between $F_{n,calc}$ and $F_{n,meas}$ for the XB-70-1 test is plotted against engine power-control-lever angle in figure 10. Each plot represents the different engine combinations (one to six engines) tested.

Figure 10 shows that, with all six engines operating and for power-control-lever angles above 35°, the calculated thrust values agree within ±2 percent of the thrust-stand measurement, with seven points at the military power setting agreeing within

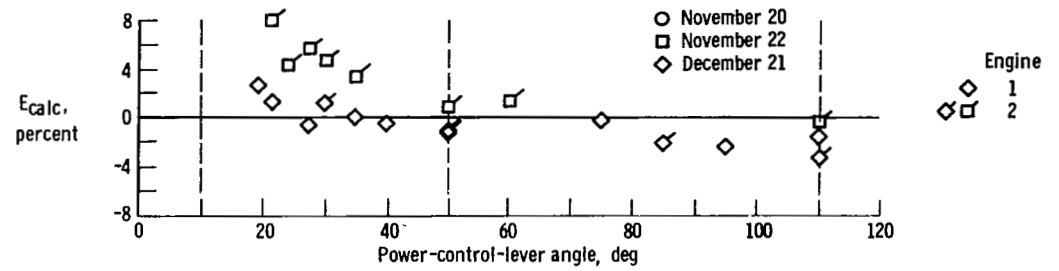

(a) One-engine runs.

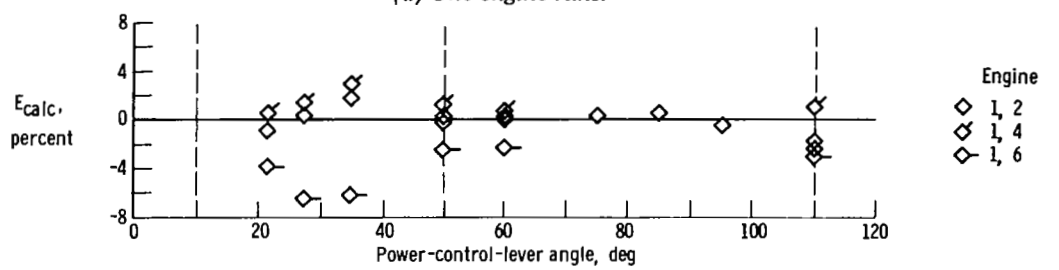

(b) Two-engine runs.

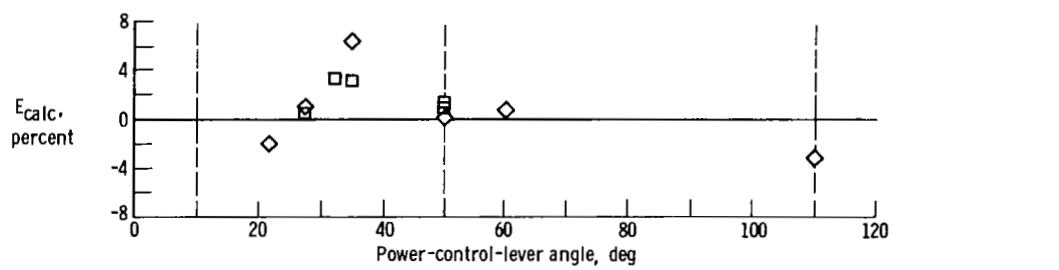

(c) Three-engine runs (engines 1, 2, and 3).

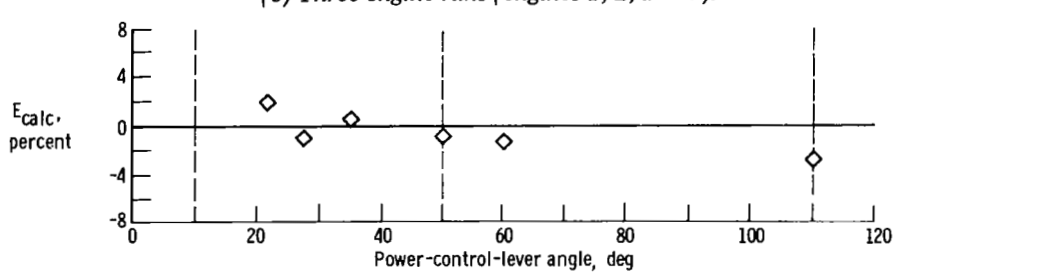

(d) Four-engine runs (engines 1, 2, 5, and 6).

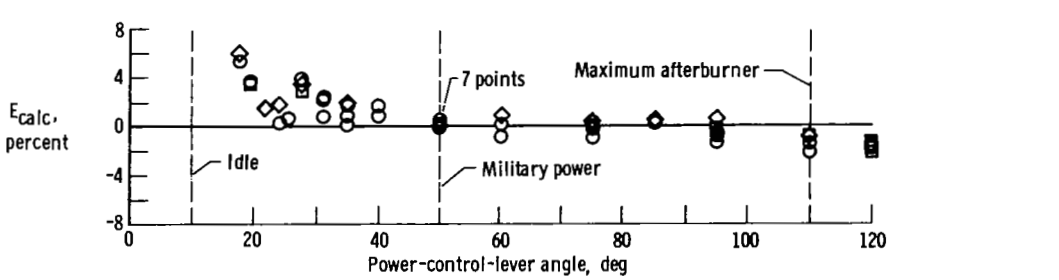

(e) Six-engine runs.

Figure 10. Variation of the calculated thrust error with power-control-lever angle and the number of engines operating.

±0.5 percent. For less than six engines operating, the agreement is within ±3.5 percent for the same range, and only as idle conditions are approached does the difference become approximately ±6 percent.

In figure 10(b), for two engines operating, data for the combination of engines 1 and 6 are in error more than data for the other two-engine combinations, because engine 6 is not as fully instrumented as engine 1 (see table 1); engine 1 $p_{t,2}$ and secondary airflow data were used in calculating the thrust of engine 6.

Except for the tests in which a lack of data is evident, figure 10 indicates that, over the entire engine power range, the six-engine tests were both the most accurate of the different engine combinations tested and had the least amount of data scatter. This trend is an indication of the instrument-error averaging and compensating effect mentioned previously.

Results from the p_7 and A_8 alternate path calculations of thrust. – The thrust values obtained by using the redundant thrust calculations of the gas generator method for the static-thrust tests are summarized in figures 11 to 13. Figure 11 shows the

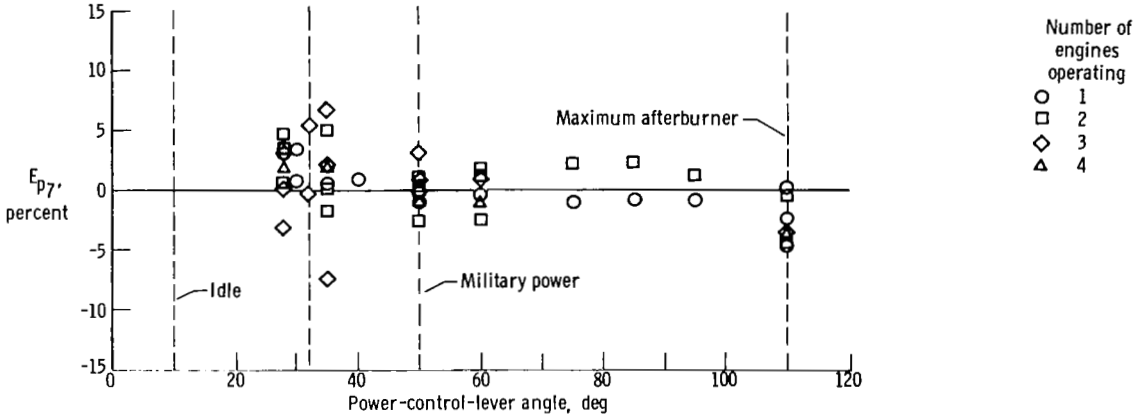

(a) Less than six-engines operating.

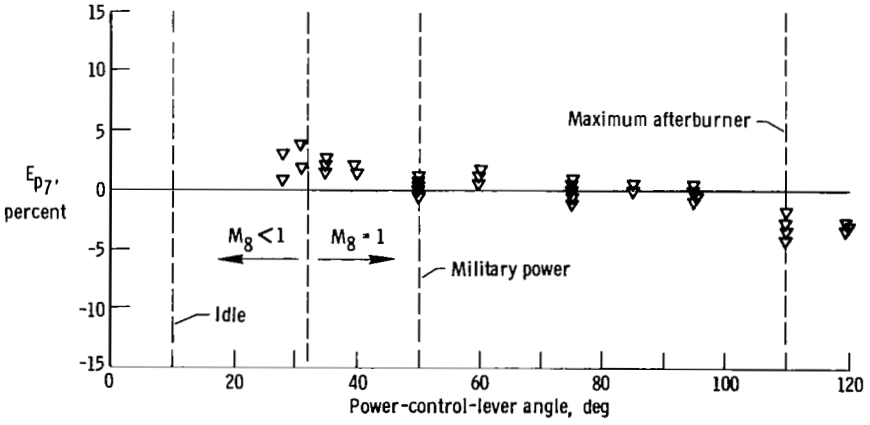

(b) Six engines operating.

Figure 11. Variation of the thrust error calculated by the p_7 path with power-control-lever angle and the number of engines operating.

percent error E_{p_7} between F_{n,p_7} and $F_{n,meas}$ plotted against engine power-control-lever angle for most of the runs that are presented in figure 10. Data for very low engine power settings are not shown because the engine airflow at station 8 for these settings (idle to 27° power-control-lever angle) was not choked and, therefore, violated the basic assumption required to calculate F_{n,p_7}. This figure also shows the average engine power-control setting where the engine airflow at station 8 becomes choked ($M_8 = 1$) for the test conditions.

Figure 12 shows the percent error E_{A_8} between F_{n,A_8} and $F_{n,meas}$ for the test data in figure 10. The A_8 alternate path method of calculating engine thrust is considered to be the most inconsistent of the three paths, because the calculating procedure is highly sensitive to any errors in the measurement of A_8. The amount of scatter and larger errors, particularly for six-engine operation, in the figure indicate this sensitivity.

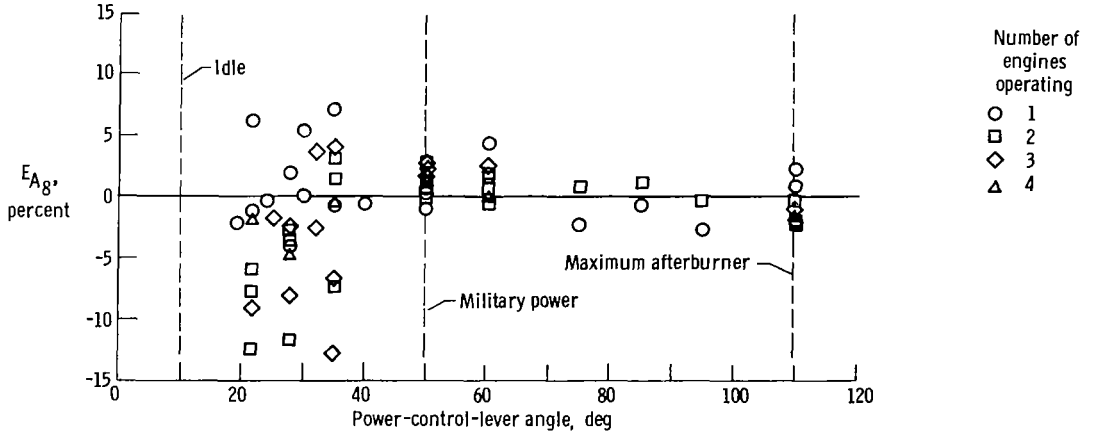

(a) Less than six engines operating.

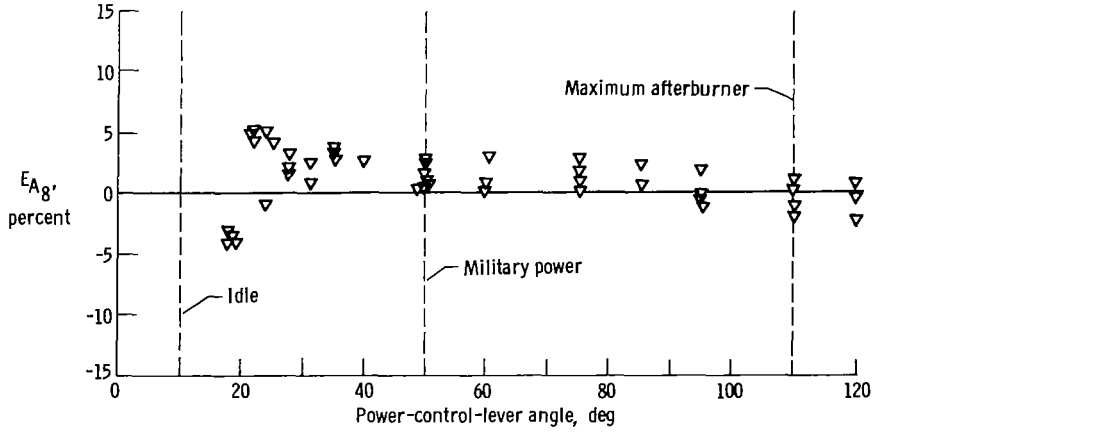

(b) Six engines operating.

Figure 12. Variation of the thrust error calculated by the A_8 path with power-control-lever angle and the number of engines operating.

The F_{n,A_8} and F_{n,p_7} paths are compared with the $F_{n,calc}$ path in figure 13 for most of the six-engine ground runs. The ratios of F_{n,p_7} and F_{n,A_8} thrust values to the thrust values calculated by the weight-flow path $F_{n,calc}$ are plotted against engine power-control-lever angles for angles of 30° and greater. This figure is presented to establish the type of relation that exists between the three different paths used by the thrust-calculating procedure and to emphasize that all three paths should be used to calculate in-flight thrust. The agreement between the three paths provides added confidence in the calculated thrust values.

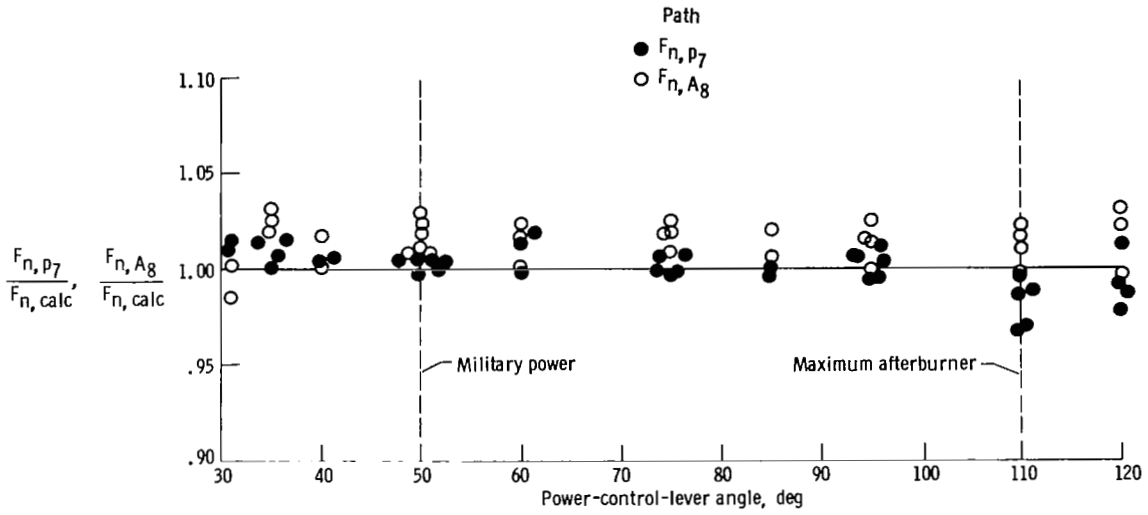

Figure 13. Ratio of the thrust values F_{n,p_7} and F_{n,A_8} to $F_{n,calc}$ for the six-engine ground runs.

From the results shown in figures 11 to 13, it can be concluded that the redundant thrust-calculating paths of the gas generator method (F_{n,p_7} and F_{n,A_8} method), although not as accurate overall as the primary thrust calculation, can serve as guidelines for investigating questionable thrust data and can be used as a backup calculation whenever the primary calculation cannot be obtained.

It should also be mentioned that a tendency for the reduction of both the thrust error and the data scatter can be seen in figures 10 to 12 as the number of engines operating increases from one to six. This characteristic is indicative of the instrument-error averaging and compensating effects that are inherent in the calculation procedure. A good example of the effectiveness of this characteristic is shown in figure 10(e) for six engines operating at the military power setting. The seven points obtained at this power setting are within ±0.5 percent of the measured thrust, an accuracy that is considerably better than the accuracy of most of the instruments that were used for the thrust calculation. The averaging characteristic also reduces the effect that a non-average engine has on the thrust calculation.

Installed Static Thrust of the YJ93-GE-3 Engine

Figure 14 shows the corrected installed engine thrust of the YJ93-GE-3 engine. Average engine corrected thrust $F_{n,k}$ is presented with and without XB-70-1 inlet losses for the six-engine runs of the ground static-thrust test as a function of engine

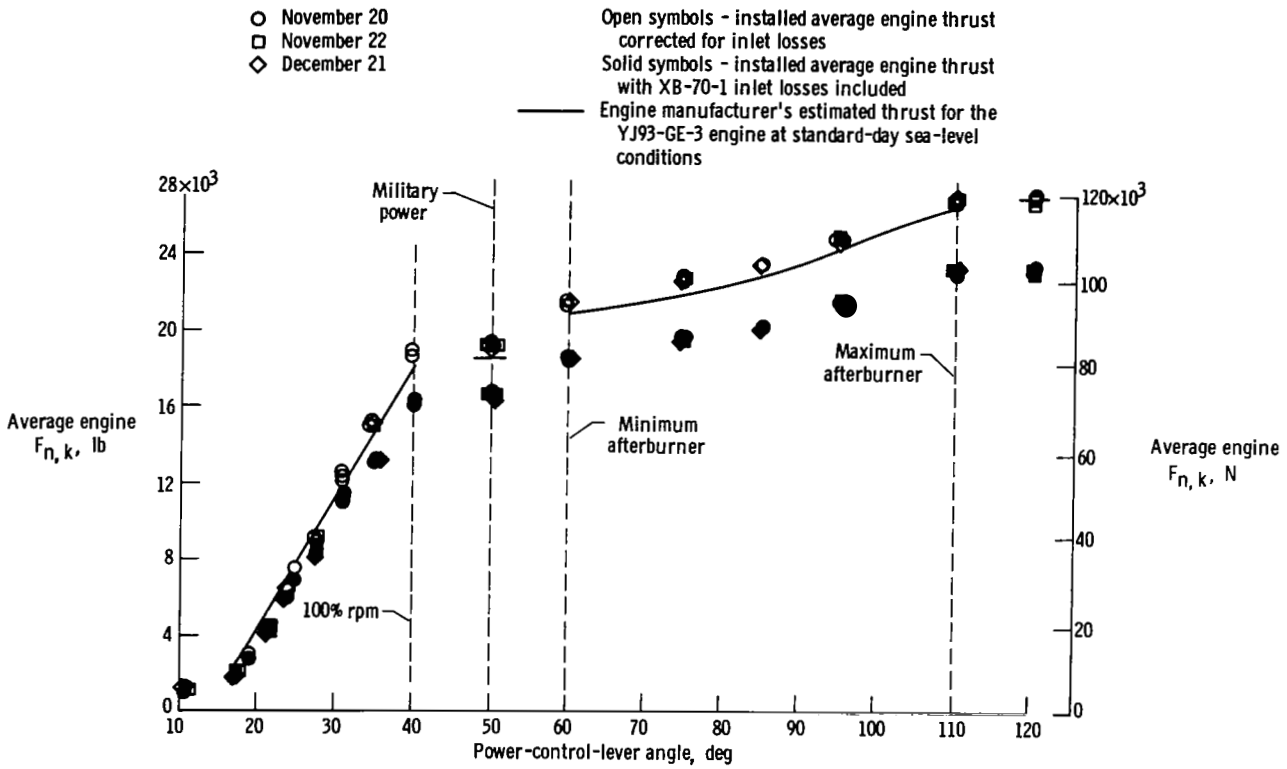

Figure 14. YJ93-GE-3 installed average engine thrust corrected to standard-day, sea-level temperature and pressure for the six-engine ground runs.

power-control-lever angle. The average engine corrected thrust was obtained from the six-engine measured thrust values $F_{n,meas}$ by using the following relations:

For thrust that includes the inlet losses

$$F_{n,k} = \frac{\frac{F_{n,meas}}{6}}{\delta_\infty} - f(T_{t,2}) \qquad (1)$$

For thrust that is corrected for inlet losses

$$F_{n,k} = \frac{\frac{F_{n,meas}}{6}}{\delta_2} - f(T_{t,2}) \qquad (2)$$

where $f(T_{t,2})$ is a sea-level, standard-day temperature correction and is a function of

the total temperature at the engine face. This correction was obtained from reference 12.

Included in figure 14 is the engine manufacturer's estimated standard-day, sea-level thrust for the YJ93-GE-3 engine. These thrust values were obtained from estimated performance curves of the YJ93-GE-3 engine included in reference 12. For power-control-lever angles greater than 35°, the engine manufacturer expected all engines to perform above these values. The estimated thrust values are for an engine operating with 7-percent secondary airflow, no "customer" bleed or power extraction, and JP-6 fuel. Although the ground static tests were not made at these exact conditions, the net effect on the thrust values is believed to be small.

The data in figure 14 show that the thrust values without the inlet losses are slightly high, as expected for power-control-lever angles above 30°, when compared with the engine manufacturer's estimated thrust curve. The average engine inlet losses shown in figure 14 are significant, for they constitute more than 13 percent of the available engine thrust for the military and all afterburner power settings. Installation losses aside from the inlet losses were not observed in this data and are believed to be small.

Inlet Tests

The effects of changes in certain inlet geometry on the in-flight thrust-calculating procedure and engine performance were obtained from several test conditions of the XB-70-1 tests. Two of these conditions — inlet throat choking tests and an inlet bypass test — involved a direct change in the inlet configuration. The procedure used to perform these tests is described in appendix C. Only the left-hand inlet was varied in the tests; this inlet and the compressor faces of engines 1, 2, and 3 were heavily instrumented for flight testing. (See table 1.)

Inlet throat choking tests. — The inlet throat choking tests were designed basically to investigate the effect of choking the airflow upstream of the engines on the reduction of the engine compressor noise (ref. 13). Inlet choking was accomplished by establishing with the engines a fixed airflow through the inlet and then reducing the inlet throat area until aerodynamic choking occurred. The effects of this test on engine performance and on the thrust-calculating procedure are shown in figure 15. The percent change in measured thrust and engine airflow, the total pressure recovery, and the difference between the test value and the initial value of the calculated thrust error E_{calc} are plotted against contraction ratio, which is the ratio of the inlet throat area to the capture area $\frac{A_t}{A_c}$. Figure 15(a) presents data for an engine speed setting of 100-percent rpm and figure 15(b), for a setting of 87-percent rpm.

The total-pressure distortion $\frac{p_{t,2_{max}} - p_{t,2_{min}}}{p_{t,2_{av}}}$ of each engine was between 9 and 11 percent for the 100-percent rpm setting and between 5 and 7 percent for the 87-percent setting. For these tests the maximum change in distortion for each engine during each test was approximately 2 percent. The contraction ratio at which the inlet choked for both test conditions is indicated in the plots.

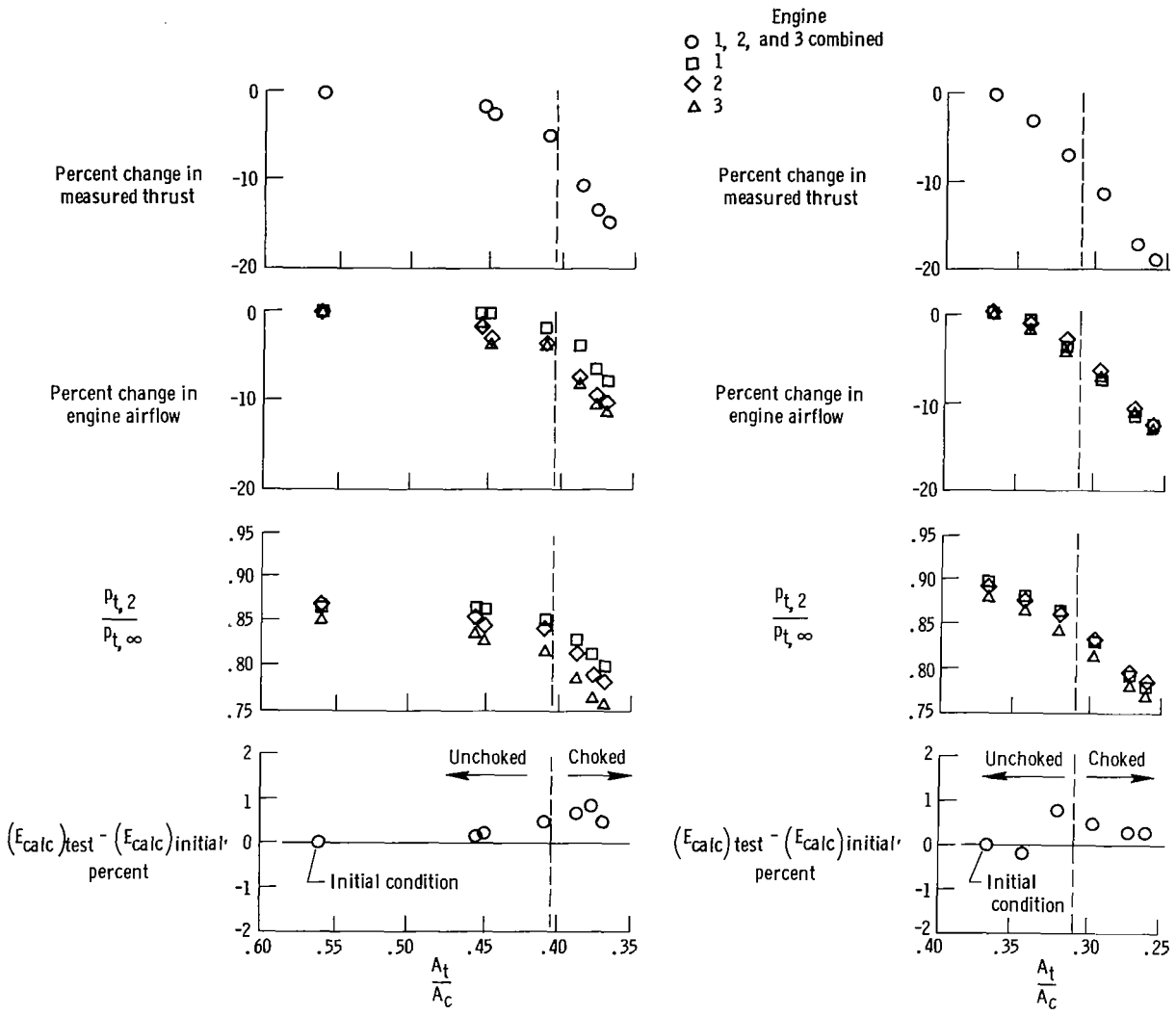

(a) Engine speed, 100-percent rpm. *(b) Engine speed, 87-percent rpm.*

Figure 15. Summary of data from the XB-70-1 left-hand inlet throat choking test. Engines 1, 2, and 3.

Although there is a significant degradation in engine thrust, the results in figure 15 show that the effect of choking the inlet on the accuracy of the thrust-calculating procedure was small; the maximum change in the net thrust error for both of the choking tests was less than 1.0 percent. This change could not be associated with any specific parameter, because of its size and because of the small quantity of data obtained from the tests, and no adverse effects were observed on any engine parameter when the inlet became choked.

Inlet bypass test. – The inlet bypass test was designed to investigate the possibility of using the bypass system as an auxiliary inlet. The test was performed by opening the bypass doors to allow additional airflow into the inlet in the manner shown in figure 16. Air flowed into a plenum surrounding the main inlet airflow path and then into the inlet through perforated duct walls. The engine secondary airflow did not enter the inlet but was used for engine cooling before it exhausted through the secondary nozzle.

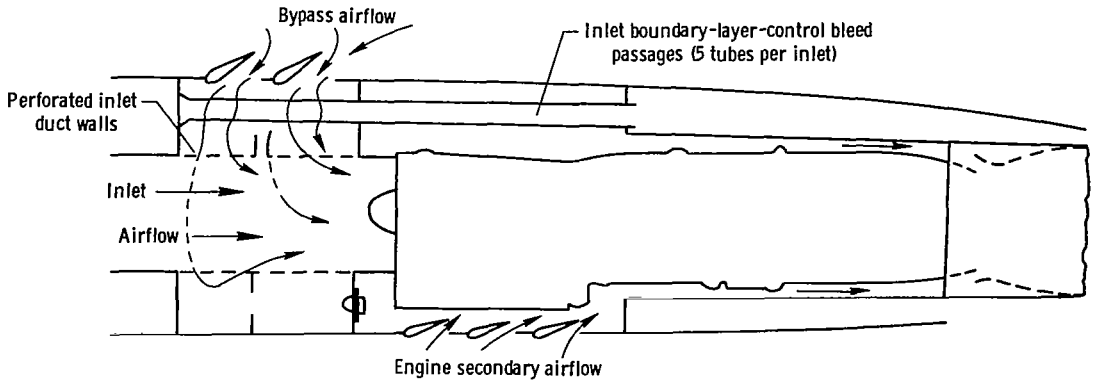

Figure 16. Schematic of engine airflow paths during the bypass test.

In addition to the expected increase in engine thrust from the additional airflow, high total-pressure distortion levels were obtained. The distortion levels increased because the airflow pattern at the face of each engine was changed by the bypass airflow entering the inlet through perforated walls just forward of the engines.

The results of this test are presented in figure 17. The percent change in the measured thrust and engine airflow, the engine face distortion D, and the difference

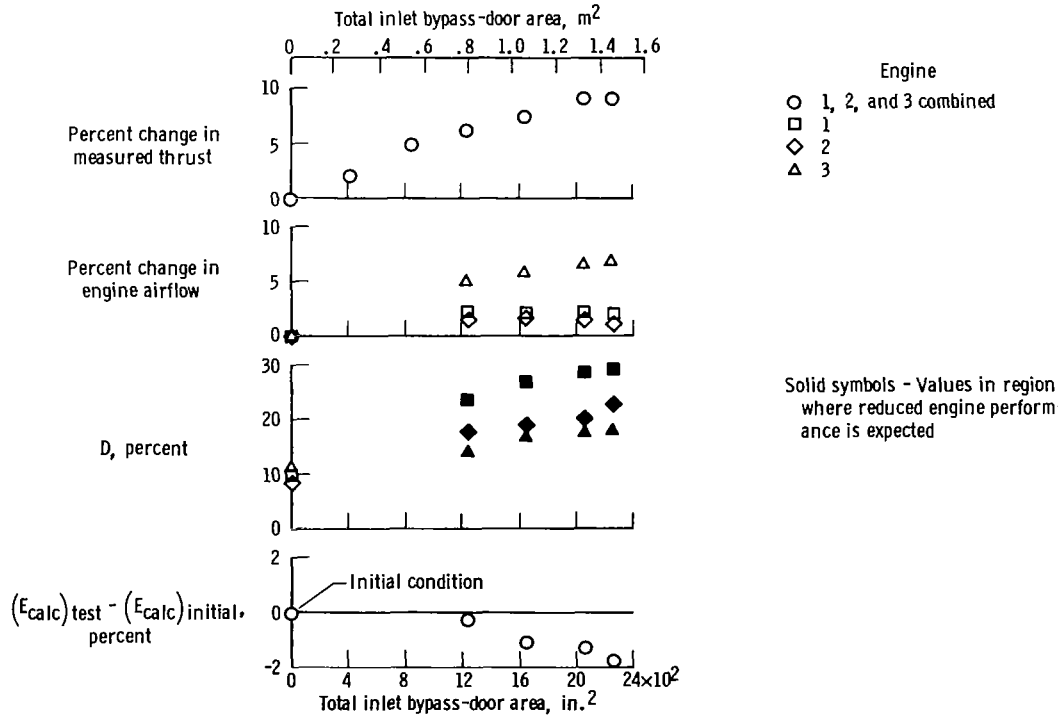

Figure 17. Summary of data from the left-hand inlet bypass test. All engines at military power setting.

between the test value and the initial value (doors closed) of the calculated net thrust error are plotted against the total inlet bypass door area. In the distortion plot, distortion values which were estimated to reduce the performance of the engine are indicated by solid symbols. This information, which was determined from a limit established by the engine manufacturer (ref. 14), is shown in figure 18. This figure shows the relationship between distortion and area ratios $\frac{A_d}{A_a}$ (ratio of an area of below-average pressure to the compressor-face annulus area) where no loss in the performance of the engine was expected.

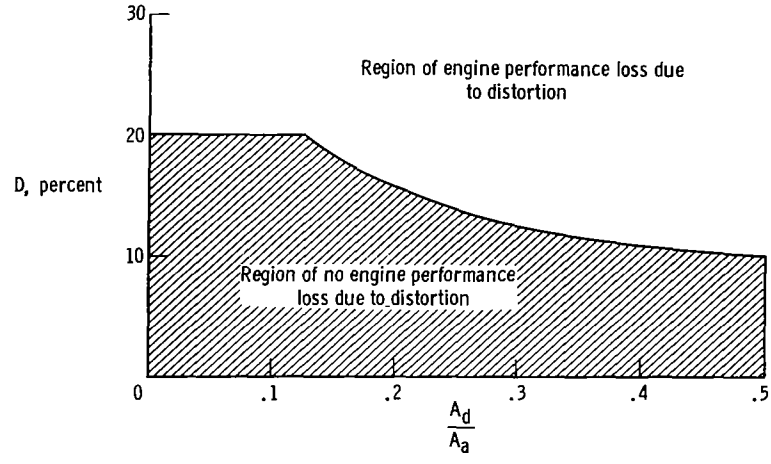

Figure 18. Maximum distortion limit for no engine performance loss for the YJ93-GE-3 engine (ref. 14) as a function of the ratio of the distorted area to the compressor-face annulus area.

The top plot of figure 17 shows that a 9-percent increase in thrust was obtained between the 0 and the 2275-inch^2 (1.468-meter^2) change in bypass-door area. Although this thrust change would recover some of the losses caused by the inlet (fig. 14), it was obtained at the expense of abnormally high distortion levels (as high as 29 percent). The bottom plot of figure 17 indicates that the high distortion levels affected the thrust-calculating procedure, in that there was a maximum change of 1.8 percent between the net thrust error at the 0 and the 2275-inch^2 (1.468-meter^2) bypass-door opening. This indication is further supported by the fact that all distortion values, other than the initial ones, are in the region where the engine performance is reduced. This is shown by the solid symbols in the distortion plot and in figure 19(a), which is discussed in the following section.

Data points for bypass-door areas between 0 and 1200 inches^2 (0.774 meter^2) were not obtained because of a malfunction in the XB-70-1 instrumentation recording package during the first part of the bypass test.

Summary of distortion levels. – Figure 19 shows the levels of distortion and their associated $\frac{A_d}{A_a}$ area ratios that were obtained in the static-thrust tests. The effects on distortion for different combinations of engines operating in the inlet duct, various inlet configurations, and conditions with engine FOD screens installed are shown. The

maximum distortion limit for no loss in engine performance (fig. 18) is shown in each of the plots of distortion versus $\frac{A_d}{A_a}$.

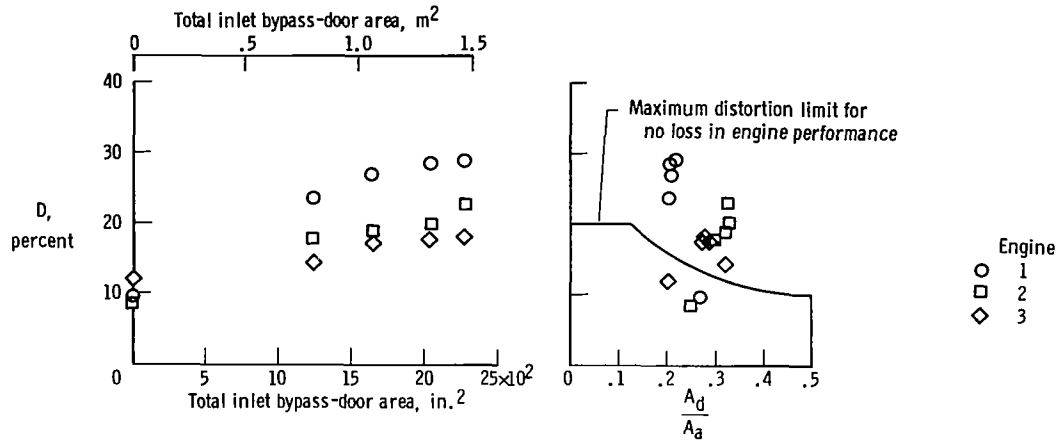

(a) Bypass test. Engine speed, 100-percent rpm.

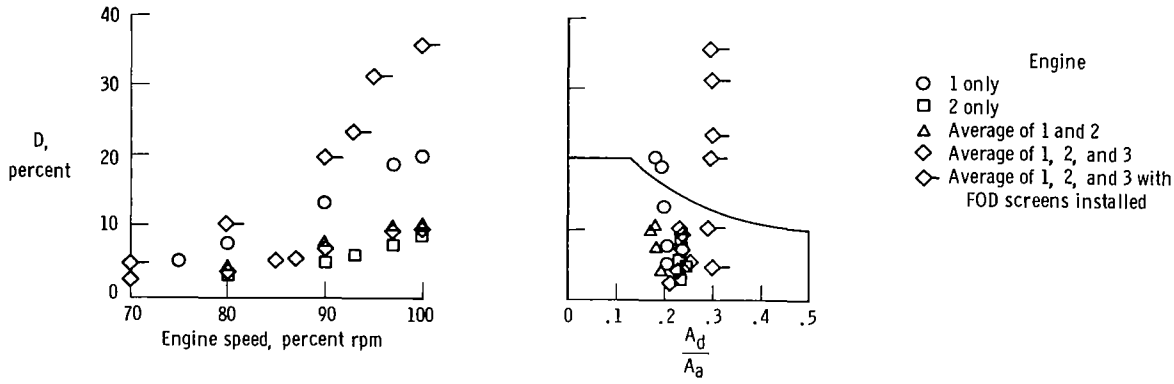

(b) Combinations of engines operating in the inlet duct.

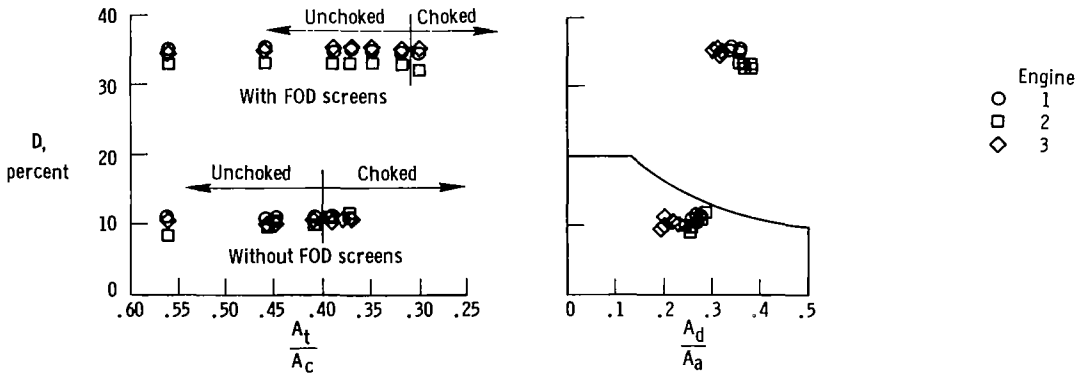

(c) Throat choking test. Engine speed, 100-percent rpm.

Figure 19. Summary of the distortion levels of left-hand inlet obtained from the tests.

Figure 19(a) shows the increase in distortion that resulted from opening the bypass doors in the inlet bypass test, which was discussed previously. The change in distortion level is shown for each of the three engines as a function of bypass-door area. The speed of the three engines in the inlet duct was maintained at 100-percent rpm throughout the entire test series. Again, as shown in the right-hand plot, opening the bypass doors caused the data to fall in the region where some loss in engine performance might be expected.

Figure 19(b) shows the change in the distortion for different combinations of engines as a function of engine speed and the effect of engine foreign object damage screens. When engine 1 is operated in the duct, higher distortion occurs, probably because of the off-center position of engine 1 and the flow through and around the nonoperating engines. FOD screens, which were used only with three engines operating, caused larger distortion and associated performance losses. However, the screens are of little consequence in flight testing because they are used only for maintenance ground runs.

Figure 19(c) shows the change in engine-face distortion level during the inlet throat choking tests. Distortion obtained for two test conditions (with and without engine FOD screens) is plotted against inlet throat contraction ratio $\frac{A_t}{A_c}$. Engine speed for both test conditions was 100-percent rpm, and the inlet was choked for points below a contraction ratio of 0.40 for the test conditions without FOD screens and 0.32 for the test conditions with FOD screens. This figure shows that inlet choking had very little effect on the engine-face distortion, but the inlet screens more than tripled the distortion.

The three plots of figure 19 show that the high distortion levels at which the performance of an engine is affected were obtained only with test conditions that would not be used in flight because of aircraft safety. These conditions included high bypass airflows entering the inlet just upstream of the engine, FOD screens installed in front of the engines, and only one engine operating in the inlet duct. It should be noted that engine thrust was not calculated for conditions with FOD screens installed because a good average for the $p_{t,2}$ measurement could not be obtained with the high levels of distortion that were experienced. This condition did provide an opportunity to examine engine performance at high distortion levels and to note that no compressor stalls were experienced for any of these abnormal conditions, which indicates that the YJ93-GE-3 engine was very tolerant of distortion.

CONCLUSIONS

A series of ground static-thrust tests was performed on the XB-70-1 airplane in a thrust-calibration facility to validate the gas generator method of calculating engine thrust and to measure the airplane engine performance. The airplane was operated with different power settings, inlet conditions, inlet flow distortions, and combinations of operating engines. The results of these tests led to the following conclusions:

1. The gas generator method of calculating jet-engine thrust determined the

engine thrust of the airplane within ±2 percent of the values measured on a thrust stand for the normal operation of six engines at power settings above 97-percent rpm (35° power-control-lever angle). At the military power setting for these conditions, all data points were within ±0.5 percent.

2. For military and higher power settings, engine thrust values calculated by two redundant thrust-calculating procedures which are built into the computer program of the gas generator method agreed within ±5 percent with all measured values. This indicates that, although the redundant calculations are not as accurate as the primary engine thrust calculation, they are accurate enough to use for investigating questionable calculated thrust data or as backup calculations whenever the thrust cannot be obtained by the primary path.

3. The influence of instrumentation errors on the thrust-calculating procedure was reduced significantly by averaging and compensating effects. This particular characteristic was most effective when large numbers of instrument measurements were used, as for the six-engine operation of the XB-70-1 airplane.

4. Results of inlet tests showed that at high total-pressure distortion levels adverse inlet conditions upstream of the engines affected the accuracy of the engine thrust calculation by a maximum of 1.8 percent.

5. For the six-engine runs of these tests, the measured thrust of an installed average engine agreed favorably with the engine manufacturer's estimated uninstalled thrust for all but the low power settings of the YJ93-GE-3 engine (idle to 87-percent rpm).

Flight Research Center,
National Aeronautics and Space Administration,
Edwards, Calif., August 12, 1970.

APPENDIX A

XB-70-1 INSTRUMENTATION USED FOR THE GROUND STATIC-THRUST TESTS

Approximately 300 XB-70-1 instrumentation parameters were used for the ground static-thrust tests. Most of these parameters, which are grouped into four types of measurements (pressure, temperature, position, and miscellaneous), are listed with their accuracy, range, and digital sampling rate in table 1. The location of the instrumentation on the airplane and engines is shown in figures 20 and 21, respectively.

Description of the Measuring Systems and Sensors

Pressure measuring system. – The XB-70-1 pressure measurements required for the static-thrust tests were made with two systems, an absolute-pressure system and a differential-pressure system. The absolute-pressure system consisted of five accurate (0.05 percent of full range) pressure transducers of the force-balance type which were kept in a controlled temperature environment. Three of the five pressures measured by the pressure transducers were used as reference pressures to the differential system. Two of these reference pressures were measured in the inlet (fig. 20), and the other was measured at the nose boom. The other two absolute pressures, free-stream static and nose-boom total, were also sensed at the nose boom.

The differential-pressure measuring system consisted of approximately 350 differential-pressure transducers positioned throughout the airplane. These transducers were of the linear variable differential transducer (LVDT) type, which measures the difference between the sensed pressure and a reference pressure so that the range of the transducer can be reduced to obtain a higher degree of accuracy. This type of transducer is designed to operate in temperature environments of up to 600° F (316° C).

Temperature measurements. – For these tests all temperature measurements on the XB-70-1 airplane, except the free-stream air total temperature, were sensed with chromel-alumel wire thermocouples. All thermocouples had the same reference junction, which was maintained at a temperature of 140° F (60° C). The free-stream air total temperature was measured by two total-temperature sensors with a dual, platinum, resistance type of temperature sensing element. Two sensors were used in order to obtain a more accurate measurement over the XB-70-1 total-temperature range; one sensor measured temperatures from -75° F to 300° F (-59° C to 149° C), and the other measured temperatures from 300° F to 700° F (149° C to 371° C). Only the low-range sensor was used for the ground static-thrust tests.

Position measurements. – All position measurements needed for the tests, except engine primary nozzle, were obtained from two types of strain-gage position measuring sensors, a bending beam and a rotary beam. The engine primary nozzle position was obtained by a "pucker string" wire that circumferentially surrounded the exit plane of the primary nozzle and was attached to a 2000-ohm potentiometer type of position sensor.

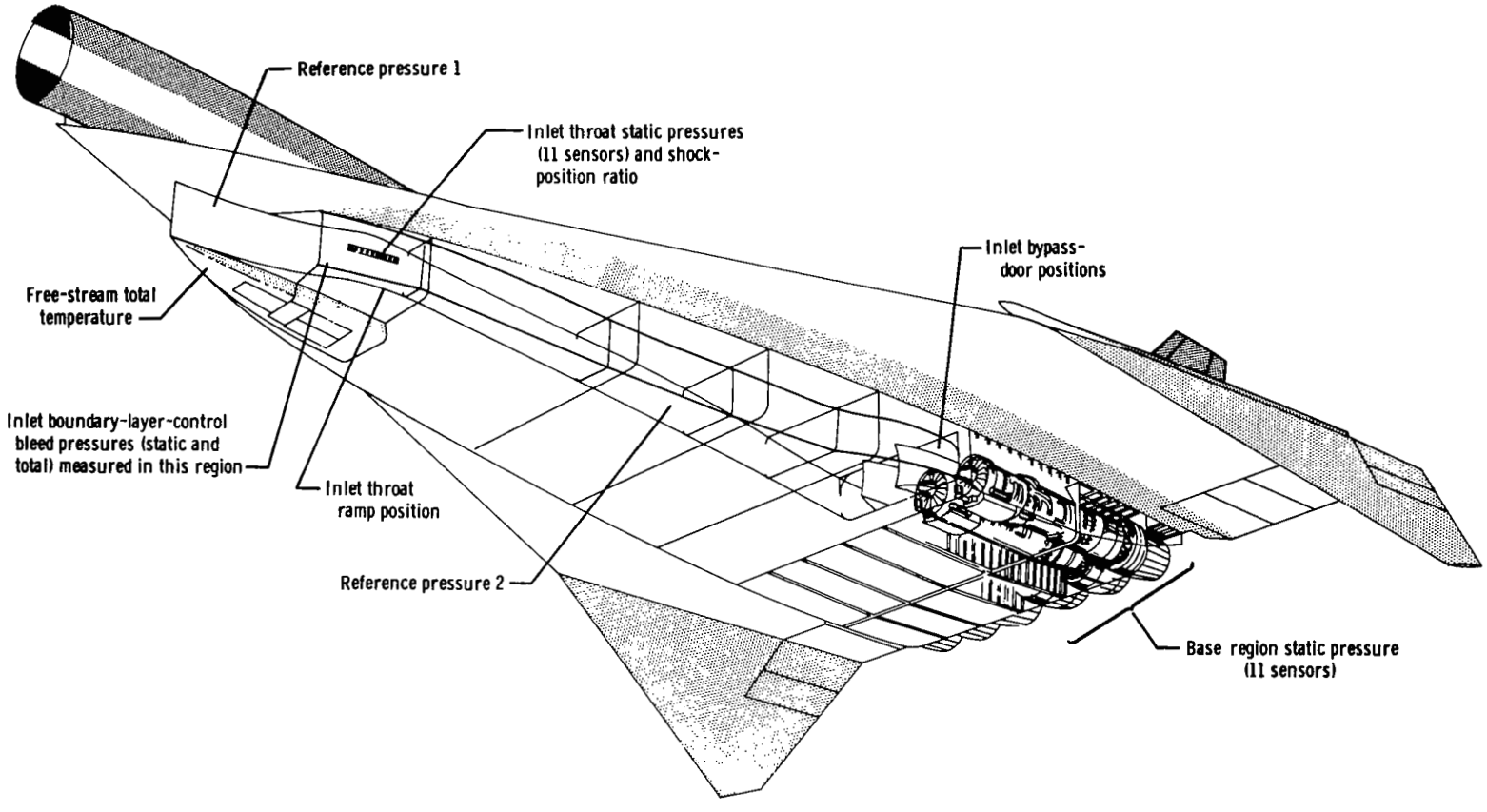

Figure 20. Location of the XB-70-1 inlet instrumentation used for the tests.

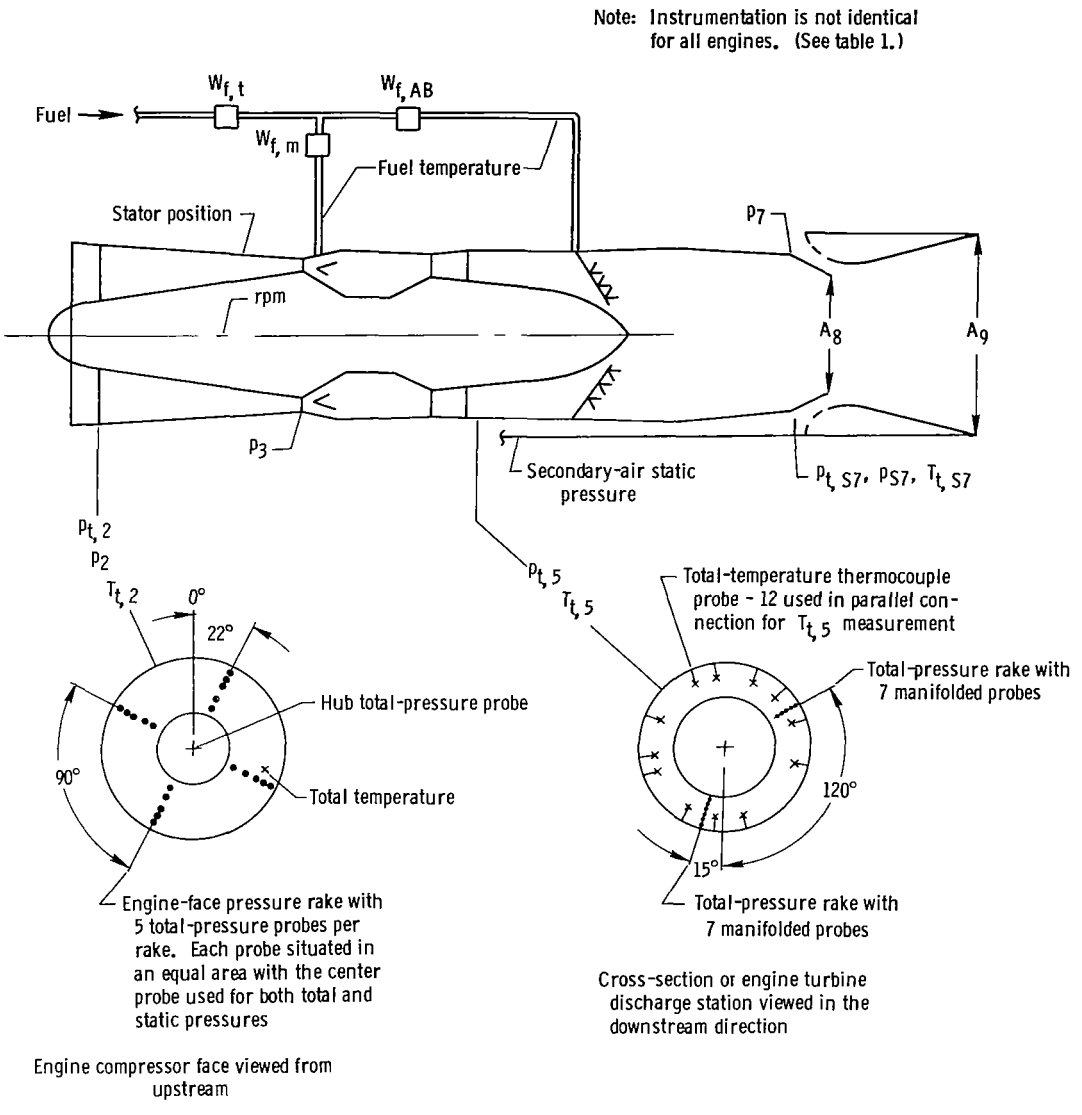

Figure 21. Location of the engine instrumentation used for the tests.

Miscellaneous measurements. – Several other aircraft sensors were used to obtain shock-position ratio, engine rpm, and engine fuel flow. Shock-position ratio was used in flight as an inlet control indicator when the inlet was started (supercritical operation). It is the ratio of a static pressure sensed downstream of the inlet terminal shock to a total pressure measured upstream of the terminal shock in the inlet throat region.

The engine fuel flow was measured in the airplane by three sensors: a main engine fuel flowmeter, an afterburner fuel flowmeter, and a total-fuel flowmeter. The main engine and afterburner flowmeters, which were of the volumetric flowmeter type, measured the volumetric rate of fuel flow with an impeller type of device. The flowmeters were located in the engine accessory pod (fig. 3). The total rate of fuel flow

entering each engine was measured by a mass flowmeter in the fuel lines upstream of the engine. The mass flowmeter measures the resistance of a flowing fluid exerted against an angular moment being applied to the fluid. The resistance is directly proportional to the mass flow rate of the fluid. With this flowmeter, measurements of the mass rate of fuel flow were not dependent on fuel temperature and specific-gravity measurements.

Instrument Calibrations

Because of the variety and the complexity of the XB-70-1 instrumentation system, a simple calibration procedure could not satisfy the calibration requirements for all the instruments. Thus a system of calibrating procedures and schedules, too complex for a detailed description here, was devised. In general, most of the instrumentation used for the static-thrust tests was calibrated in either a laboratory or an installed position in the airplane (some instruments used both) and was checked out for zero shifts a few hours before the tests and at the beginning of each test day prior to engine start.

Two methods were used to calibrate the installed instruments. One was a physical simulation of the quantity to be measured, for example, pressure applied to the absolute-pressure sensors. The other was a simulation of the electrical signal output of the sensor. Both methods were used on many of the instruments.

Telemetered Data

The XB-70-1 airborne instrumentation system had provisions for radio transmission of 36 aircraft instrumentation parameters. During these tests, 26 of the 36 channels were used to transmit inlet duct pressure and engine power-control-lever data to the NASA Flight Research Center control room. At this facility, pressures across the inlet duct walls were observed during the throat choking test to prevent structural damage to the airplane when low static pressures in the inlet duct were encountered.

APPENDIX B

EXTERNAL INSTRUMENTATION AND TEST APPARATUS USED FOR THE XB-70-1 GROUND STATIC-THRUST TESTS

Aircraft Static-Thrust Calibration Facility

The Edwards Air Force Base aircraft static-thrust calibration facility was designed to measure and record both the static thrust and the weight of a test aircraft. The facility consists of four large, structural-steel, loading platforms and a control room in an underground reinforced-concrete structure. The load platforms, which are mounted flush with the surface, form the pit roof. The platforms are installed in the form of a cross; the number designation is shown in figure 5. The underground control room is near the left end of platform 1.

Description of the platform assembly. – Figure 22 is a schematic drawing of the side and end views of platform 1. The other three platforms are constructed similarly. Each platform assembly is suspended from the reinforced-concrete structure by four vertical flexure straps attached to two horizontal support beams. The flexure straps are connected to both the support beam and the pit structure by pins to insure a minimum of friction in the fore and aft movement of the platform.

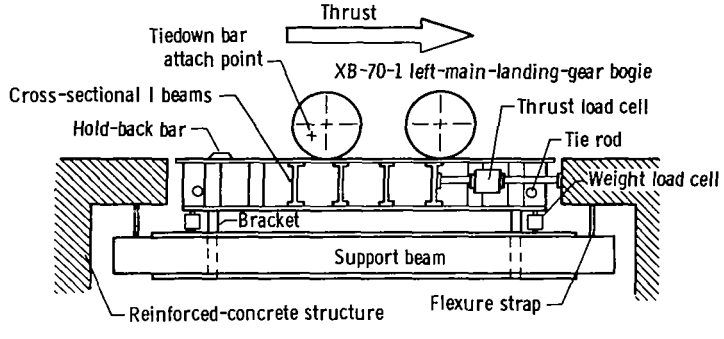

(a) Right side view.

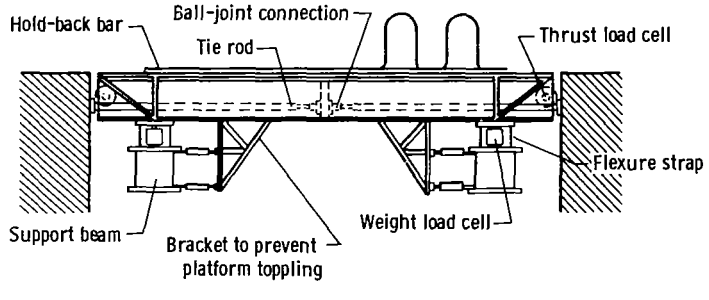

(b) End view, looking forward.

Figure 22. Schematic drawing of platform 1 assembly of the static-thrust calibration facility.

APPENDIX B

The loading platform is supported by four weight load cells of the strain-gage type which are incorporated into the flexure-strap support-beam assembly. Each platform can measure up to 300,000 pounds (1,334,000 newtons) of vertical force.

Thrust loads are measured by two thrust load cell assemblies which are horizontally attached to the platform and pit structure near each front corner of the platform. The thrust load cells are of a special, precision, strain-gage type capable of measuring thrust loads on each platform from a negative 62,500 pounds (278,000 newtons) to a positive 125,000 pounds (556,000 newtons).

Lateral forces on a platform are resisted by two horizontal tie rods in the fore and aft sections of the platform. The tie rods, which are attached to the pit structure and a platform center member, are perpendicular to the line of thrust and were designed so that they would not affect the thrust or weight forces on the platform assembly.

Four brackets, attached to both the loading platform and the support beams, prevent the platform from overturning.

Control room and recording equipment. – Electrical signals obtained from the thrust and weight load cells are transmitted to a console in the main section of the control room. (See fig. 23.) Thrust and weight loads are recorded separately on strip-chart

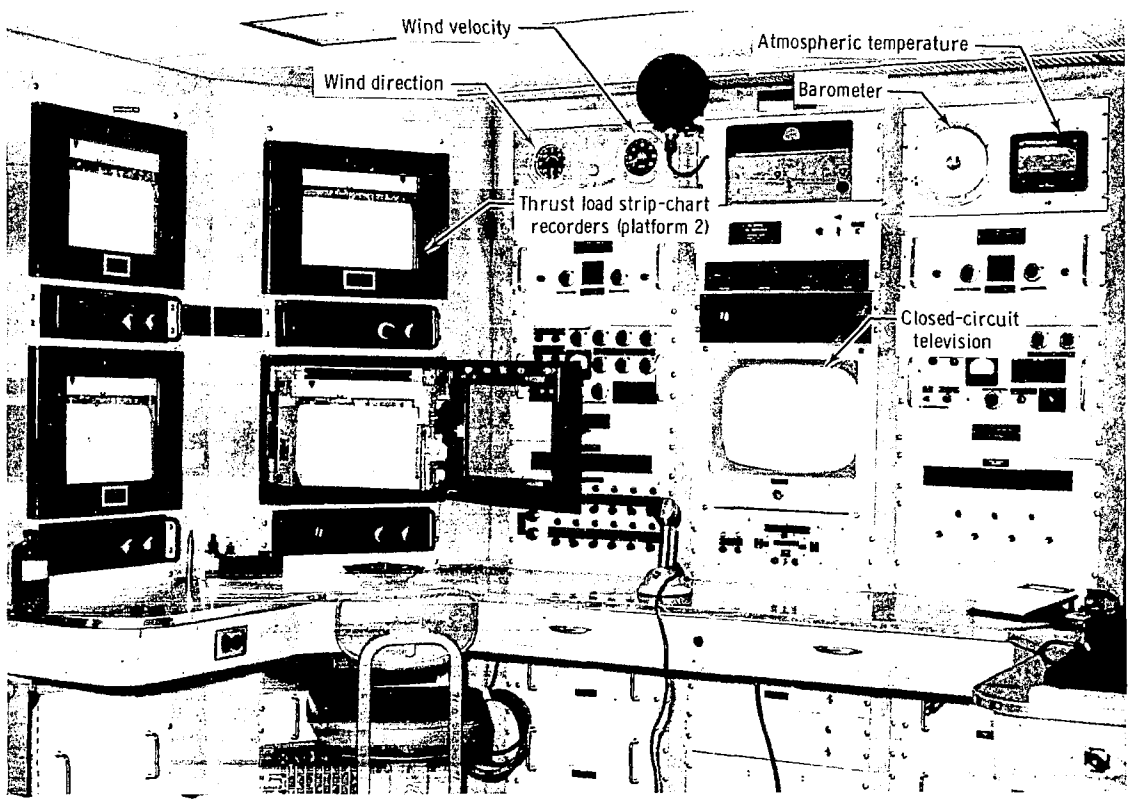

E-19324

Figure 23. Control room of the static-thrust calibration facility.

recorders for each platform. Each strip-chart recorder has a range-changing mechanism which may be automatically or manually operated. The ranges of the thrust recorders are shown in the following table:

Range number	Thrust polarity	Thrust value,	
		lb	N
1	Forward	0 to 10,000	0 to 44,480
2	Forward	10,000 to 20,000	44,480 to 88,960
3	Forward	20,000 to 60,000	88,960 to 266,900
4	Forward	60,000 to 100,000	266,900 to 444,800
5	Forward	100,000 to 140,000	444,800 to 622,700
-1	Reverse	10,000 to 0	44,480 to 0
-2	Reverse	20,000 to 10,000	88,960 to 44,480
-3	Reverse	60,000 to 20,000	266,900 to 88,960

The ranges for the weight recorders are shown in the following table:

Range number	Weight value,	
	lb	N
1	0 to 10,000	0 to 44,480
2	10,000 to 20,000	44,480 to 88,960
3	0 to 100,000	0 to 444,800
4	100,000 to 200,000	444,800 to 889,600
5	200,000 to 300,000	889,600 to 1,334,000

In addition to the strip-chart recorders, the thrust and weight loads can be totalized for one platform or for any combination of the four platforms. This value is displayed on an electronic digital light panel. Incorporated into this system is a data-acquisition system with a printout of time, total thrust, and total weight on a flexowriter typewriter with a tape punch.

In addition to the recording and indicating instrumentation, a closed-circuit television system permits monitoring of the test aircraft during a thrust calibration. Wind direction and velocity, outside-air temperature, and barometric-pressure indicators were installed to determine ambient conditions at the thrust calibration stand. Radio communication is provided between the test aircraft and the control room.

Calibration and accuracies for the ground static-thrust tests of the XB-70-1 airplane. - The weight measuring devices of the static-thrust measuring facility were not used in the ground static-thrust tests of the XB-70-1 airplane; therefore, only the calibration methods and accuracies of the thrust measuring instruments will be discussed. The thrust measuring instruments on each platform are calibrated with a Revere super precision, 100,000-pound capacity, universal load cell with a Revere model R-100 digital force indicator. This calibration unit has an accuracy of 0.01 percent of reading or 25 pounds (111 newtons), whichever is greater. The calibration of this unit is directly traceable to the National Bureau of Standards.

APPENDIX B

In normal calibration procedures, forces are applied at the center of the aft edge of each platform. Asymmetric load calibrations were also performed for these tests, because the XB-70-1 landing gear rested near the edges of platforms 1 and 2. (See figs. 5 and 22.)

Results from previous calibrations and calibrations made before and after the XB-70-1 tests (including asymmetric load calibrations) showed that the accuracy of each platform was ±100 pounds (±445.8 newtons) for thrust loads from 0 to 20,000 pounds (88,960 newtons) and ±250 pounds (±1112 newtons) for thrust loads from 20,000 pounds (88,960 newtons) to 125,000 pounds (556,000 newtons). Much of the increase in error at 20,000 pounds (88,960 newtons) and at greater loads was caused by the range-changing mechanism of the strip-chart recorder as the scale changed from range 2 to range 3.

Miscellaneous Instrumentation

External measurement of fuel flow. – To calibrate the internal fuel-flow measuring system of the XB-70-1 airplane in its installed position, the engine fuel flow was measured by a special, external fuel-flow measuring system. The flow was measured for engines 1, 2, and 3 during the ground runs and for engines 4, 5, and 6 during the inlet sweep runs. The system, designed by the engine manufacturer, consisted of an external fuel-line loop installed in the fuel line upstream of the engine from which the fuel flow was to be measured. Each loop contained a thermocouple with an accuracy of ±2.0° F (±1.11° C) and two accurate fuel-flow meters (±0.5 percent of reading) of the volumetric type. These measurements were recorded in the control room of the thrust-calibration facility. This system measured only the total fuel being consumed by each engine.

Meteorological measurements. – Most of the meteorological data for these tests were obtained from the Edwards Air Force Base, Detachment 21, 6th Weather Wing, Air Weather Service. Atmospheric temperature, pressure, and relative humidity experienced during the tests are presented in table 2.

Additional meteorological measurements were made on two of the testing days (November 16 and December 21) with a 50-foot (15.24-meter) tower located approximately 800 feet (243.8 meters) to the left of the XB-70-1 airplane. Wind velocity and direction, temperatures, and relative humidity were sensed at heights of 6 feet and 50 feet (1.83 meters and 15.24 meters). These data were used for the noise-evaluation study, which was part of the overall ground-test investigation. The wind velocities and directions in table 2 were obtained from the aircraft static-thrust calibration facility. These measurements were taken approximately 50 feet (15.24 meters) from the left wing of the airplane at a height of 6 feet (1.83 meters).

Fuel specific-gravity measurements. – The specific gravity of the fuel in the XB-70 airplane for these tests was measured by a Baumé type of hydrometer with a scale from 0.70 to 1.00 and an accuracy within ±0.5 percent of the nominal reading. The temperature of the fuel was also measured with each specific-gravity measurement to obtain an accurate value for fuel density.

APPENDIX C

XB-70-1 GROUND STATIC-THRUST TESTS AND TEST RUNS

The XB-70-1 airplane was secured to the loading platforms of the aircraft static-thrust calibration facility by two tiedown fixtures, one on each of the main-landing-gear bogies (fig. 5). The landing-gear struts were fully extended to level the airplane and prevent any change in attitude during the test.

To prevent damage to the inlet from a large change in pressure across the inlet-duct wall during the throat choking tests, two of the four boundary-layer-control bleed regions of each inlet were blocked.

Ground support equipment consisted of gasoline-driven hydraulic, electrical, and air-conditioner units. The units were beneath the airplane but, at all times, off the loading platforms which were being used to record thrust (fig. 8).

Because the objectives of the XB-70-1 ground static-thrust tests were so unrelated in many respects, several independent tests were devised to meet all the test requirements. The test conditions required were as follows:

Inlet sweep runs - The inlet sweep runs were designed primarily to clear the left-hand inlet of any foreign objects which might damage the XB-70-1 engines during the inlet throat choking and bypass tests and to check out the instrumentation. The runs were performed in the following manner:

1. FOD screens were installed on all six engines.

2. With engines 1, 2, and 3 at 100-percent rpm power setting and the inlet throat at full open, the bypass doors of the left-hand inlet were opened in incremental steps from 0 to full open at 2285 inches^2 (1.474 meters^2) combined door area.

3. With the bypass doors closed and the engine settings the same as in item 2, the left-hand-inlet throat area was reduced until the inlet airflow at the throat became choked.

Normal six-engine operation - The test conditions for normal six-engine operations were as follows:

1. Bypass doors were closed and inlet throat settings were at the full-open position.

2. All engines were at the same power setting for each run.

3. Engine power settings were varied from idle to 120° in incremental steps.

Different combinations of operating engines - Different engine combinations were used primarily to obtain engine noise as a function of the distance between operating engines. The six-engine runs discussed in the preceding section overlapped this condition. Engine power setting varied from idle to maximum afterburner; the

requirements for the inlet settings were the same as for the six-engine operation. The different combinations of operating engines were as follows:

1. Engines 1, 2, 5, and 6.

2. Engines 1, 2, and 3.

3. Engines 1 and 6.

4. Engines 1 and 4.

5. Engines 1 and 2.

6. Engine 2 only.

7. Engine 1 only.

Inlet throat choking test - The throat choking test was designed to determine the reduction in engine compressor noise and the resultant propulsion system performance loss from choking the inlet airflow upstream of the engines. The test conditions were as follows:

1. Airflow was established through the inlet duct, and the variable inlet throat area was reduced until the flow became choked.

2. The left-hand-inlet duct was used with engines 1, 2, and 3 operating. The inlet was choked at two conditions, military power and 87-percent-rpm setting. The bypass doors were closed throughout the test.

Inlet bypass test - The test conditions for the inlet bypass test, which was designed to investigate engine-face distortion with a simulated secondary inlet, were as follows:

1. The left-hand-inlet bypass doors were opened in incremental steps from 0 to 2275-inch^2 (1.468-meter^2) combined door area to allow airflow to enter the inlet and engines by way of the bypass-door openings and through the perforated duct wall. (See fig. 16.)

2. The left-hand inlet was used only with engines 1, 2, and 3 operating at military power, and the inlet throat area was held constant at the full-open position.

Miscellaneous tests - Additional tests were performed as follows:

1. Engines 4, 5, and 6 were operated from idle to 120° power settings (in incremental steps) with the external fuel-flow measuring system.

2. With engines 1 and 3 at military power, engine 2 was reduced from military power to 80-percent rpm in incremental steps.

The runs performed in the ground static-thrust tests are listed in table 2.

TABLE 2. RUNS OF THE XB-70-1 GROUND STATIC-THRUST TEST.

(a) Inlet sweep runs performed on November 16, 1967.

Time of day, hr:min:sec	Run no.	Power-control-lever angle, deg						Left-inlet setting			Measured thrust,		Temperature,		Pressure,		Relative humidity, percent	Wind		
		Engine						Bypass area,		Throat area ratio A_t/A_c								Velocity,		Direction, deg
		1	2	3	4	5	6	in^2	m^2		lb	N	deg F	deg C	lb/in^2	N/m^2		knots	m/sec	
12:25:02	1	Off	Off	Off	11.0	11.0	11.0	Closed	Closed	0.56	2,905	12,900	71.0	21.7	13.56	93,490	31	0	0.0	---
28:26	2	↓	↓	↓	17.5	17.5	17.5	Closed	Closed	.56	5,125	22,800	71.0	21.7	13.56	93,490	31	7	3.5	0
31:16	3				21.5	21.5	21.5	Closed	Closed	.56	10,330	45,950	71.0	21.7	13.56	93,490	31	7	3.5	0
34:17	4				27.5	27.5	27.5	Closed	Closed	.56	19,110	95,000	71.0	21.7	13.56	93,490	31	5	2.5	30
37:01	5				30.5	30.5	30.5	Closed	Closed	.56	23,270	103,500	71.5	21.9	13.56	93,490	31	4	2.0	40
40:01	6				35.0	35.0	35.0	Closed	Closed	.56	30,140	134,050	71.5	21.9	13.56	93,490	30	2	1.0	350
42:45	7				50.0	50.0	50.0	Closed	Closed	.56	38,020	169,100	71.5	21.9	13.56	93,490	30	0	0.0	---
44:40	8				60.0	60.0	60.0	Closed	Closed	.56	42,215	187,800	72.0	22.2	13.56	93,490	30	0	0.0	---
46:09	9				75.0	75.0	75.0	Closed	Closed	.56	44,615	198,450	72.0	22.2	13.56	93,490	30	0	0.0	---
47:42	10				85.0	85.0	85.0	Closed	Closed	.56	46,220	205,600	72.0	22.2	13.56	93,490	30	0	0.0	---
49:02	11				95.0	95.0	95.0	Closed	Closed	.56	48,390	215,250	72.0	22.2	13.56	93,490	30	0	0.0	---
50:30	12				110.0	110.0	110.0	Closed	Closed	.56	51,430	228,800	72.0	22.2	13.56	93,490	30	0	0.0	---
52:01	13	↓	↓	↓	120.0	120.0	120.0	Closed	Closed	.56	51,935	231,050	72.0	22.2	13.56	93,490	29	0	0.0	---
53:40	14	110.0	110.0	110.0	110.0	110.0	110.0	Closed	Closed	.56	101,895	453,250	72.0	22.2	13.56	93,490	29	7	3.5	350
14:03:08	15	40.0	40.0	40.0	Off	Off	Off	Closed	Closed	.56	36,370	161,800	74.0	23.3	13.56	93,490	34	3	1.5	350
05:16	16	40.0	40.0	40.0				410	0.26	.56	36,950	164,350	74.0	23.3	13.56	93,490	34	1	0.5	30
08:23	17	40.0	40.0	40.0				835	0.54	.56	37,380	166,300	74.0	23.3	13.56	93,490	34	1	0.5	30
10:15	18	40.0	40.0	40.0				1250	0.81	.56	38,390	170,800	74.0	23.3	13.56	93,490	34	1	0.5	30
12:07	19	40.0	40.0	40.0				1650	1.06	.56	38,270	170,250	74.0	23.3	13.56	93,490	34	7	3.5	90
13:48	19A	40.0	40.0	40.0				2045	1.32	.56	38,480	171,150	74.0	23.3	13.56	93,490	35	7	3.5	90
15:32	20	40.0	40.0	40.0				2285	1.47	.56	38,595	171,700	74.0	23.3	13.56	93,490	35	7	3.5	90
18:00	21	40.0	40.0	40.0				Closed	Closed	.56	36,370	161,800	74.0	23.3	13.56	93,490	35	7	3.5	90
20:39	22	40.0	35.0	40.0				Closed	Closed	.56	34,535	153,600	74.0	23.3	13.56	93,490	35	7	3.5	90
23:00	23	40.0	27.5	40.0				Closed	Closed	.56	30,640	136,300	74.0	23.3	13.56	93,490	35	7	3.5	90
24:26	24	40.0	21.5	40.0				Closed	Closed	.56	28,525	126,900	74.0	23.3	13.56	93,490	36	7	3.5	90
28:00	25	40.0	17.5	40.0				Closed	Closed	.56	27,225	121,100	74.0	23.3	13.56	93,490	36	7	3.5	90
30:14	26	40.0	11.0	40.0				Closed	Closed	.56	26,975	120,000	73.5	23.1	13.56	93,490	36	7	3.5	90
36:48	27	40.0	40.0	40.0				Closed	Closed	.56	36,225	161,150	73.5	23.1	13.56	93,490	36	9	4.5	0
41:07	28	40.0	40.0	40.0				Closed	Closed	.46	35,930	159,850	73.5	23.1	13.56	93,490	36	9	4.5	0
42:44	29	40.0	40.0	40.0				Closed	Closed	.44	35,630	158,500	73.5	23.1	13.56	93,490	37	9	4.5	0
44:29	30	40.0	40.0	40.0				Closed	Closed	.42	35,410	157,500	73.0	22.8	13.56	93,490	37	9	4.5	0
46:12	31	40.0	40.0	40.0				Closed	Closed	.39	34,725	154,450	73.0	22.8	13.56	93,490	37	9	4.5	0
47:48	32	40.0	40.0	40.0				Closed	Closed	.37	33,995	151,200	73.0	22.8	13.56	93,490	37	9	4.5	0
50:15	33	40.0	40.0	40.0				Closed	Closed	.35	32,885	146,300	73.0	22.8	13.56	93,490	37	9	4.5	0
52:20	34	40.0	40.0	40.0				Closed	Closed	.32	30,865	137,300	73.0	22.8	13.56	93,490	37	9	4.5	0
53:35	35	40.0	40.0	40.0	↓	↓	↓	Closed	Closed	.30	28,255	125,700	73.0	22.8	13.56	93,490	37	9	4.5	0

TABLE 2. Continued.

(b) Static ground runs performed on November 20, 1967.

Time of day, hr:min:sec	Run no.	Power-control-lever angle, deg						Left-inlet setting			Measured thrust,		Temperature,		Pressure,		Relative humidity, percent	Wind		
		Engine						Bypass area,		Throat area ratio A_t/A_c								Velocity,		Direction, deg
		1	2	3	4	5	6	in^2	m^2		lb	N	deg F	deg C	lb/in^2	N/m^2		knots	m/sec	
9:52:30	27	11.0	11.0	11.0	11.0	11.0	11.0	Closed	Closed	0.56	6,380	28,400	54.0	12.2	13.58	93,630	73	8	4.1	340
57:50	28	17.5	17.5	17.5	17.5	17.5	17.5	Closed	Closed	.56	11,385	50,650	54.0	12.2	13.58	93,630	72	4	2.1	350
10:00:45	29	21.5	21.5	21.5	21.5	21.5	21.5	Closed	Closed	.56	23,510	104,600	54.0	12.2	13.58	93,630	72	5	2.6	340
02:30	30	24.0	24.0	24.0	24.0	24.0	24.0	Closed	Closed	.56	33,630	149,600	54.0	12.2	13.58	93,630	72	4	2.1	10
06:50	30A	25.5	25.5	25.5	25.5	25.5	25.5	Closed	Closed	.56	38,585	171,600	54.5	12.5	13.58	93,630	72	4	2.1	10
09:30	31	27.5	27.5	27.5	27.5	27.5	27.5	Closed	Closed	.56	46,620	207,400	54.5	12.5	13.58	93,630	71	5	2.6	10
12:30	32	35.0	35.0	35.0	35.0	35.0	35.0	Closed	Closed	.56	74,020	329,250	54.5	12.5	13.58	93,630	71	6	3.1	8
14:50	33	50.0	50.0	50.0	50.0	50.0	50.0	Closed	Closed	.56	93,065	413,950	54.5	12.5	13.58	93,630	71	6	3.1	0
17:20	34	60.0	60.0	60.0	60.0	60.0	60.0	Closed	Closed	.56	103,900	462,150	55.0	12.8	13.58	93,630	71	4	2.1	10
18:35	35	75.0	75.0	75.0	75.0	75.0	75.0	Closed	Closed	.56	109,225	485,850	55.0	12.8	13.58	93,630	71	5	2.6	0
20:20	36	85.0	85.0	85.0	85.0	85.0	85.0	Closed	Closed	.56	113,520	504,950	55.0	12.8	13.58	93,630	71	4	2.1	0
22:30	37	95.0	95.0	95.0	95.0	95.0	95.0	Closed	Closed	.56	119,900	533,350	55.0	12.8	13.58	93,630	71	4	2.1	0
23:50	38	110.0	110.0	110.0	110.0	110.0	110.0	Closed	Closed	.56	128,940	573,550	55.0	12.8	13.58	93,630	71	4	2.1	355
25:00	39	120.0	120.0	120.0	120.0	120.0	120.0	Closed	Closed	.56	129,760	577,200	55.5	13.1	13.58	93,630	71	5	2.6	350
33:40	40	11.0	11.0	11.0	11.0	11.0	11.0	Closed	Closed	.56	6,285	27,950	56.0	13.3	13.58	93,630	70	5	2.6	350
37:30	41	19.2	19.2	19.2	19.2	19.2	19.2	Closed	Closed	.56	16,240	72,250	56.0	13.3	13.58	93,630	70	5	2.6	05
41:00	42	31.1	31.1	31.1	31.1	31.1	31.1	Closed	Closed	.56	61,225	272,350	56.0	13.3	13.58	93,630	70	6	3.1	0
44:30	43	40.0	40.0	40.0	40.0	40.0	40.0	Closed	Closed	.56	90,725	403,550	56.0	13.3	13.58	93,630	70	5	2.6	15
46:30	44	50.0	50.0	50.0	50.0	50.0	50.0	Closed	Closed	.56	92,985	413,600	56.5	13.6	13.58	93,630	70	0	0	---
48:32	45	75.0	75.0	75.0	75.0	75.0	75.0	Closed	Closed	.56	109,790	488,350	56.5	13.6	13.58	93,630	70	6	3.1	10
50:30	46	95.0	95.0	95.0	95.0	95.0	95.0	Closed	Closed	.56	119,835	533,050	56.5	13.6	13.58	93,630	70	5	2.6	10
51:50	47	110.0	110.0	110.0	110.0	110.0	110.0	Closed	Closed	.56	128,650	272,250	56.5	13.6	13.58	93,630	69	8	4.1	340
53:35	48	120.0	120.0	120.0	120.0	120.0	120.0	Closed	Closed	.56	129,645	576,700	56.5	13.6	13.58	93,630	69	9	4.6	05
55:25	49	95.0	95.0	95.0	95.0	95.0	95.0	Closed	Closed	.56	119,670	532,300	57.0	13.9	13.58	93,630	69	6	3.1	10
57:20	50	75.0	75.0	75.0	75.0	75.0	75.0	Closed	Closed	.56	110,165	490,050	57.0	13.9	13.58	93,630	69	6	3.1	20
11:00:10	51	50.0	50.0	50.0	50.0	50.0	50.0	Closed	Closed	.56	93,400	415,450	57.0	13.9	13.57	93,560	69	7	3.6	15
39:00	52	11.0	11.0	11.0	11.0	11.0	11.0	Closed	Closed	.56	6,250	27,800	57.5	14.2	13.57	93,560	71	8	4.1	350
42:10	53	31.1	31.1	31.1	31.1	31.1	31.1	Closed	Closed	.56	60,285	268,160	58.0	14.4	13.57	93,560	71	5	2.6	350
44:50	54	35.0	35.0	35.0	35.0	35.0	35.0	Closed	Closed	.56	73,330	326,200	58.0	14.4	13.57	93,560	71	6	3.1	15
11:47:15	55	40.0	40.0	40.0	40.0	40.0	40.0	Closed	Closed	.56	89,925	400,000	58.0	14.4	13.57	93,560	71	6	3.1	25
49:35	56	50.0	50.0	50.0	50.0	50.0	50.0	Closed	Closed	.56	92,600	411,900	58.0	14.4	13.57	93,560	71	4	2.1	20
53:15	57	60.0	60.0	60.0	60.0	60.0	60.0	Closed	Closed	.56	102,855	457,500	58.0	14.4	13.57	93,560	71	9	4.6	30
54:10	58	50.0	50.0	50.0	50.0	50.0	50.0	Closed	Closed	.56	92,370	410,900	58.0	14.4	13.57	93,560	72	8	4.1	20
56:45	59	35.0	35.0	35.0	35.0	35.0	35.0	Closed	Closed	.56	73,315	326,100	58.0	14.4	13.57	93,560	72	5	2.6	350
12:00:10	60	31.1	31.1	31.1	Off	Off	Off	Closed	Closed	.56	61,855	275,150	58.0	14.4	13.56	93,490	72	2	1.0	45
25:30	73	50.0	50.0	50.0	↓	↓	↓	Closed	Closed	.56	45,160	200,900	58.5	14.7	13.56	93,490	68	5	2.6	30
27:07	74	50.0	50.0	50.0	↓	↓	↓	415	0.268	.56	46,060	204,900	58.5	14.7	13.56	93,490	68	0	0	---
28:40	75	50.0	50.0	50.0	↓	↓	↓	840	0.54	.56	47,115	209,600	58.5	14.7	13.56	93,490	68	8	4.1	30
30:00	76	50.0	50.0	50.0	↓	↓	↓	1245	0.803	.56	47,810	215,000	58.5	14.7	13.56	93,490	68	6	3.1	30
31:50	77	50.0	50.0	50.0	↓	↓	↓	1645	1.06	.56	48,475	215,600	58.5	14.7	13.56	93,490	68	8	4.1	0
33:50	77A	50.0	50.0	50.0	↓	↓	↓	2045	1.319	.56	48,880	217,400	58.5	14.7	13.56	93,490	68	8	4.1	30
35:30	78	50.0	50.0	50.0	↓	↓	↓	2275	1.47	.56	49,060	218,200	58.5	14.7	13.56	93,490	68	8	4.1	25
37:46	79	50.0	35.0	50.0	↓	↓	↓	Closed	Closed	.56	42,565	189,350	58.5	14.7	13.56	93,490	67	7	3.6	20
38:55	80	50.0	27.5	50.0	↓	↓	↓	Closed	Closed	.56	39,085	173,850	58.5	14.7	13.56	93,490	67	7	3.6	20
40:20	81	50.0	21.5	50.0	↓	↓	↓	Closed	Closed	.56	35,235	156,750	59.0	15.0	13.56	93,490	66	8	4.1	30

TABLE 2. Continued.

(c) Static ground runs performed on November 22, 1967.

Time of day, hr:min:sec	Run no.	Power-control-lever angle, deg						Left-inlet setting			Measured thrust,		Temperature,		Pressure,		Relative humidity, percent	Wind		
		Engine						Bypass area,		Throat area ratio A_t/A_c								Velocity,		Direction, deg
		1	2	3	4	5	6	in^2	m^2		lb	N	deg F	deg C	lb/in^2	N/m^2		knots	m/sec	
7:26:03	83A	27.5	27.5	27.5	Off	Off	Off	Closed	Closed	0.56	24,600	109,450	49.0	9.4	13.54	93,360	71	7	3.6	20
28:47	83B	32.3	32.3	32.3	↓	↓	↓	Closed	Closed	.56	33,310	148,200	49.0	9.4	13.54	93,360	71	7	3.6	17
31:22	83C	35.0	35.0	35.0	↓	↓	↓	Closed	Closed	.56	37,445	166,550	49.0	9.4	13.55	93,420	71	7.5	3.9	25
33:44	84	50.0	50.0	50.0	↓	↓	↓	Closed	Closed	.56	47,350	210,600	49.0	9.4	13.55	93,420	71	6.5	3 3	20
35:44	85	50.0	50.0	50.0	↓	↓	↓	Closed	Closed	.457	46,500	206,805	49.0	9.4	13.55	93,420	71	8	4.1	20
37:00	86	50.0	50.0	50.0	↓	↓	↓	Closed	Closed	.453	45,975	204,500	49.5	9.7	13.55	93,420	71	5	2.6	10
38:32	87	50.0	50.0	50.0	↓	↓	↓	Closed	Closed	.409	45,055	200,400	49.5	9.7	13.55	93,420	71	6.5	3.3	50
40:25	88	50.0	50.0	50.0	↓	↓	↓	Closed	Closed	.389	42,780	190,300	49.5	9.7	13.55	93,420	71	6.5	3.3	15
42:16	88A	50.0	50.0	50.0	↓	↓	↓	Closed	Closed	.377	41,025	182,450	50.0	10.0	13.55	93,420	71	8	4.1	10
44:08	88B	50.0	50.0	50.0	↓	↓	↓	Closed	Closed	.370	40,395	179,700	50.0	10.0	13.55	93,420	71	5	2.6	12
49:05	90	35.0	35.0	35.0	↓	↓	↓	Closed	Closed	.370	33,685	149,850	50.0	10.0	13.55	93,420	71	7	3.6	7
51:45	91	32.3	32.3	32.3	↓	↓	↓	Closed	Closed	.370	30,640	136,300	50.0	10.0	13.55	93,420	71	7	3.6	10
55:00	92	27.5	27.5	27.5	↓	↓	↓	Closed	Closed	.370	23,400	104,100	50.0	10.0	13.55	93,420	71	5.5	2.8	5
58:05	93	25.5	25.5	25.5	↓	↓	↓	Closed	Closed	.370	19,450	86,500	50.5	10.3	13.55	93,420	71	6	3.1	10
8:00:59	93A	25.5	25.5	25.5	↓	↓	↓	Closed	Closed	.345	18,855	83,850	50.5	10.3	13.55	93,420	71	6	3.1	7
12:10	94	25.5	25.5	25.5	↓	↓	↓	Closed	Closed	.324	18,135	80,605	51.0	10.6	13.55	93,420	70	6	3.1	5
14:03	95	25.5	25.5	25.5	↓	↓	↓	Closed	Closed	.300	17,230	76,650	51.0	10.6	13.55	93,420	70	6	3.1	10
16:45	96	25.5	25.5	25.5	↓	↓	↓	Closed	Closed	.279	16,165	71,900	51.0	10.6	13.55	93,420	69	6	3.1	00
18:34	97	25.5	25.5	25.5	↓	↓	↓	Closed	Closed	.275	15,825	70,400	51.0	10.6	13.55	93,420	69	5	2.6	2
21:21	99	25.5	25.5	25.5	↓	↓	↓	Closed	Closed	.281	16,185	72,000	51.0	10.6	13.55	93,420	69	2.5	1.3	7
23:34	100	25.5	25.5	25.5	↓	↓	↓	Closed	Closed	.324	18,220	81,050	51.0	10.6	13.55	93,420	69	2	1.0	280
25:18	101	25.5	25.5	25.5	↓	↓	↓	Closed	Closed	.365	19,165	85,250	51.0	10.6	13.56	93,490	68	0	0	---
44:54	61	27.5	27.5	27.5	27.5	27.5	27.5	Closed	Closed	.56	48,065	213,800	51.0	10.6	13.56	93,490	66	4.5	2.3	345
48:01	62	21.5	21.5	21.5	21.5	21.5	21.5	Closed	Closed	.56	24,155	107,450	51.5	10.8	13.56	93,490	65	5.5	2.8	352
51:00	63	17.5	17.5	17.5	17.5	17.5	17.5	Closed	Closed	.56	11,665	51,900	51.5	10.8	13.56	93,490	65	6	3.1	0
53:58	64	11.0	11.0	11.0	11.0	11.0	11.0	Closed	Closed	.56	6,370	28,350	51.5	10.8	13.56	93,490	65	5.5	2.8	345
56:34	65	50.0	50.0	50.0	50.0	50.0	50.0	Closed	Closed	.56	94,235	419,200	51.5	10.8	13.56	93,490	65	7	3.6	340
59:18	66	120.0	120.0	120.0	120.0	120.0	120.0	Closed	Closed	.56	130,680	581,300	51.5	10.8	13.56	93,490	64	4	2.1	335
9:00:47	67	110.0	110.0	110.0	110.0	110.0	110.0	Closed	Closed	.56	131,080	58,350	51.5	10.8	13.56	93,490	64	4	2.1	330
9:03:32	68	95.0	95.0	95.0	95.0	95.0	95.0	Closed	Closed	.56	121,550	540,700	51.5	10.8	13.56	93,490	64	4.5	2.3	338
04:23	69	75.0	75.0	75.0	75.0	75.0	75.0	Closed	Closed	.56	111,080	494,100	51.5	10.8	13.56	93,490	64	1.5	0.8	70
07:08	70	50.0	50.0	50.0	50.0	50.0	50.0	Closed	Closed	.56	94,875	422,000	51.5	10.8	13.56	93,490	63	3.5	1.8	335
09:11	71	110.0	110.0	110.0	110.0	110.0	110.0	Closed	Closed	.56	131,005	582,750	51.5	10.8	13.56	93,490	63	2	1.0	215
10:41	72	120.0	120.0	120.0	120.0	120.0	120.0	Closed	Closed	.56	130,970	582,600	51.5	10.8	13.56	93,490	63	0	0	---
21:42	116	Off	11.0	Off	Off	Off	Off	Closed	Closed	.56	1,030	4,600	51.0	10.6	13.56	93,490	62	3.5	1.8	345
23:54	117	↓	21.5	↓	↓	↓	↓	Closed	Closed	.56	3,795	16,900	51.0	10.6	13.56	93,490	62	4	2.1	05
26:00	118	↓	27.5	↓	↓	↓	↓	Closed	Closed	.56	8,165	36,300	51.0	10.6	13.56	93,490	62	4.5	2.3	340
28:14	119	↓	30.3	↓	↓	↓	↓	Closed	Closed	.56	10,345	46,000	51.0	10.6	13.56	93,490	62	2.5	1.3	335
30:11	120	↓	35.0	↓	↓	↓	↓	Closed	Closed	.56	14,060	62,550	51.0	10.6	13.56	93,490	61	4.5	2.3	348
32:16	121	↓	50.0	↓	↓	↓	↓	Closed	Closed	.56	18,685	83,100	51.0	10.6	13.55	93,420	61	4.5	2.3	355
33:29	122	↓	60.0	↓	↓	↓	↓	Closed	Closed	.56	20,790	92,500	51.0	10.6	13.55	93,420	61	5	2.6	12
34:43	123	↓	110.0	↓	↓	↓	↓	Closed	Closed	.56	26,055	115,900	51.0	10.6	13.55	93,420	61	5	2.6	23
37:20	124	↓	24.0	↓	↓	↓	↓	Closed	Closed	.56	6,775	30,100	51.0	10.6	13.55	93,420	61	2.5	1.3	350

TABLE 2. Concluded.

(d) Static ground runs performed on December 21, 1967.

Time of day, hr:min:sec	Run no.	Power-control-lever angle, deg						Left-inlet setting			Measured thrust,		Temperature,		Pressure,		Relative humidity, percent	Wind		
		Engine						Bypass area,		Throat area ratio A_t/A_c								Velocity,		Direction, deg
		1	2	3	4	5	6	in^2	m^2		lb	N	deg F	deg C	lb/in^2	N/m^2		knots	m/sec	
5:08:18	1	11.0	Off	Off	Off	Off	Off	Closed	Closed	0.56	1,100	4,800	26.0	-3.3	13.67	94,250	77	0	0	---
11:12	2	35.0						Closed	Closed	.56	15,790	70,250	26.0	-3.3	13.67	94,250	77	2	1.0	0
13:27	3	50.0						Closed	Closed	.56	19,620	87,250	26.0	-3.3	13.67	94,250	77	3	1.5	0
14:59	4	95.0						Closed	Closed	.56	24,635	109,500	26.0	-3.3	13.67	94,250	77	3	1.5	0
16:14	5	110.0						Closed	Closed	.56	26,785	119,150	25.5	-3.6	13.67	94,250	77	0	0	---
17:36	6	75.0						Closed	Closed	.56	22,785	101,350	25.5	-3.6	13.67	94,250	77	0	0	---
19:11	7	40.0						Closed	Closed	.56	18,745	83,400	25.5	-3.6	13.67	94,250	77	0	0	---
21:40	9	27.5						Closed	Closed	.56	10,215	45,450	25.5	-3.6	13.67	94,250	77	1	0.5	0
24:03	11	21.5						Closed	Closed	.56	4,920	21,900	25.5	-3.6	13.67	94,250	77	3	1.5	0
26:31	12	19.2						Closed	Closed	.56	3,340	14,850	25.5	-3.6	13.67	94,250	77	4	2.1	0
33:24	13	11.0					11.0	Closed	Closed	.56	2,230	9,900	25.0	-3.9	13.68	94,320	77	0	0	---
36:05	14	21.5					21.5	Closed	Closed	.56	9,795	43,550	25.0	-3.9	13.68	94,320	77	1	0.5	350
38:29	15	27.5					27.5	Closed	Closed	.56	21,110	93,900	25.0	-3.9	13.68	94,320	77	2	1.0	330
40:56	16	35.0					35.0	Closed	Closed	.56	32,690	145,400	25.0	-3.9	13.68	94,320	77	2	1.0	330
43:14	17	50.0					50.0	Closed	Closed	.56	40,200	178,800	25.0	-3.9	13.68	94,320	77	4	2.1	0
44:48	18	60.0					60.0	Closed	Closed	.56	44,110	196,200	25.0	-3.9	13.68	94,320	77	3	1.5	30
46:10	19	110.0					110.0	Closed	Closed	.56	55,110	245,150	25.0	-3.9	13.68	94,320	77	0	0	---
53:18	20	11.0			11.0		Off	Closed	Closed	.56	1,930	8,600	25.0	-3.9	13.68	94,320	77	0	0	---
55:44	21	21.5			21.5			Closed	Closed	.56	9,630	42,850	25.0	-3.9	13.68	94,320	77	3	1.5	0
58:14	22	27.5			27.5			Closed	Closed	.56	20,365	90,600	25.0	-3.9	13.68	94,320	77	3	1.5	0
6:00:38	23	35.0			35.0			Closed	Closed	.56	31,130	138,450	25.0	-3.9	13.68	94,320	77	4	2.1	0
02:53	24	50.0			50.0			Closed	Closed	.56	39,065	173,750	25.0	-3.9	13.69	94,390	77	3	1.5	0
04:22	25	60.0			60.0			Closed	Closed	.56	43,425	193,150	25.0	-3.9	13.69	94,390	77	3	1.5	0
05:39	26	110.0			110.0			Closed	Closed	.56	55,000	244,650	25.0	-3.9	13.69	94,390	77	3	1.5	0
27:08	27	11.0	11.0	11.0	11.0	11.0	11.0	Closed	Closed	.56	6,780	30,150	24.5	-4.2	13.69	94,390	77	0	0	---
30:42	28	17.5	17.5	17.5	17.5	17.5	17.5	Closed	Closed	.56	12,940	57,550	24.5	-4.2	13.69	94,390	77	0	0	---
33:28	29	21.5	21.5	21.5	21.5	21.5	21.5	Closed	Closed	.56	27,520	122,400	24.0	-4.4	13.69	94,390	77	4	2.1	0
36:11	30	24.0	24.0	24.0	24.0	24.0	24.0	Closed	Closed	.56	38,485	171,200	24.0	-4.4	13.69	94,390	77	4	2.1	0
38:53	31	27.5	27.5	27.5	27.5	27.5	27.5	Closed	Closed	.56	53,860	234,600	24.0	-4.4	13.69	94,390	77	4	2.1	0
41:45	32	35.0	35.0	35.0	35.0	35.0	35.0	Closed	Closed	.56	80,405	357,650	24.0	-4.4	13.69	94,390	77	4	2.1	0
44:10	33	50.0	50.0	50.0	50.0	50.0	50.0	Closed	Closed	.56	101,795	452,800	24.0	-4.4	13.69	94,390	77	4	2.1	315
45:59	34	60.0	60.0	60.0	60.0	60.0	60.0	Closed	Closed	.56	112,440	500,400	24.0	-4.4	13.70	94,460	77	4	2.1	330
47:31	35	75.0	75.0	75.0	75.0	75.0	75.0	Closed	Closed	.56	118,370	526,550	24.0	-4.4	13.70	94,460	77	4	2.1	330
49:03	36	85.0	85.0	85.0	85.0	85.0	85.0	Closed	Closed	.56	122,705	545,800	24.0	-4.4	13.70	94,460	77	4	2.1	330
50:32	37	95.0	95.0	95.0	95.0	95.0	95.0	Closed	Closed	.56	129,390	575,550	24.0	-4.4	13.70	94,460	77	2	1.0	320
6:52:50	38	110.0	110.0	110.0	110.0	110.0	110.0	Closed	Closed	.56	139,700	621,550	24.0	-4.4	13.70	94,460	77	2	1.0	320
59:17	125	11.0	11.0	11.0	Off	Off	Off	Closed	Closed	.56	3,375	15,000	24.0	-4.4	13.70	94,460	77	0	0	---
7:02:07	126	21.5	21.5	21.5				Closed	Closed	.56	13,320	59,250	24.0	-4.4	13.70	94,460	77	0	0	---
04:41	127	27.5	27.5	27.5				Closed	Closed	.56	26,840	119,400	24.0	-4.4	13.70	94,460	76	5	2.6	0
07:16	128	35.0	35.0	35.0				Closed	Closed	.56	38,305	170,400	24.0	-4.4	13.70	94,460	76	5	2.6	0
09:37	129	50.0	50.0	50.0				Closed	Closed	.56	50,460	224,450	24.0	-4.4	13.70	94,460	76	6	3.1	0
11:11	130	60.0	60.0	60.0				Closed	Closed	.56	55,720	247,850	24.0	-4.4	13.70	94,460	76	5	2.6	0
12:33	131	110.0	110.0	110.0				Closed	Closed	.56	70,825	315,100	24.5	-4.2	13.70	94,460	76	4	2.1	0
23:18	102	11.0	11.0	Off				Closed	Closed	.56	2,255	10,050	25.0	-3.9	13.71	94,530	74	5	2.6	0
26:51	103	21.5	21.5					Closed	Closed	.56	9,025	40,150	25.0	-3.9	13.71	94,530	74	5	2.6	0
29:22	104	27.5	27.5					Closed	Closed	.56	18,625	82,850	25.0	-3.9	13.71	94,530	74	6	3.1	0
32:04	105	35.0	35.0					Closed	Closed	.56	28,670	127,550	25.0	-3.9	13.71	94,530	73	6	3.1	0
34:22	106	50.0	50.0					Closed	Closed	.56	37,375	166,250	25.0	-3.9	13.71	94,530	73	6	3.1	0
35:48	107	60.0	60.0					Closed	Closed	.56	41,165	316,550	25.0	-3.9	13.71	94,530	73	6	3.1	0
37:11	108	110.0	110.0					Closed	Closed	.56	51,710	230,000	25.0	-3.9	13.71	94,530	72	6	3.1	0
49:59	109	11.0	11.0			11.0	11.0	Closed	Closed	.56	4,560	20,300	25.5	-3.6	13.72	94,600	71	4	2.1	0
53:02	110	21.5	21.5			21.5	21.5	Closed	Closed	.56	18,615	82,800	25.5	-3.6	13.72	94,600	70	6	3.1	0
55:28	111	27.5	27.5			27.5	27.5	Closed	Closed	.56	34,100	173,900	26.0	-3.3	13.72	94,600	70	6	3.1	15
58:20	112	35.0	35.0			35.0	35.0	Closed	Closed	.56	58,540	260,400	26.0	-3.3	13.72	94,600	69	6	3.1	0
9:00:40	113	50.0	50.0			50.0	50.0	Closed	Closed	.56	75,855	337,400	26.0	-3.3	13.73	94,670	69	7	3.6	0
02:30	114	60.0	60.0			60.0	60.0	Closed	Closed	.56	84,170	374,400	26.0	-3.3	13.73	94,670	69	8	4.1	0
03:53	115	110.0	110.0			110.0	110.0	Closed	Closed	.56	105,025	467,150	26.0	-3.3	13.73	94,670	69	8	4.1	0
11:56	119	Off	30.3			Off	Off	Closed	Closed	.56	11,845	52,700	26.5	-3.1	13.73	94,670	69	5	2.6	0
14:20	121		50.0					Closed	Closed	.56	19,965	888,000	27.0	-2.8	13.73	94,670	69	6	3.1	0
18:02	123		110.0					Closed	Closed	.56	27,825	123,750	27.0	-2.8	13.73	94,670	68	6	3.1	0
19:35	132		85.0					Closed	Closed	.56	24,335	108,250	27.0	-2.8	13.73	94,670	68	6	3.1	0
21:59	133		50.0					Closed	Closed	.56	19,920	88,600	27.0	-2.8	13.73	94,670	68	6	3.1	0
24:24	134		11.0					Closed	Closed	.56	1,135	5,050	27.0	-2.8	13.73	94,670	68	7	3.6	0
33:31	33A	50.0	50.0					Closed	Closed	.56	36,925	164,250	27.5	-2.5	13.73	94,670	67	6	3.1	0
35:27	34A	60.0	60.0					Closed	Closed	.56	41,045	182,600	27.5	-2.5	13.73	94,670	67	6	3.1	0
36:58	35A	75.0	75.0					Closed	Closed	.56	42,640	189,650	28.0	-2.2	13.73	94,670	67	8	4.1	0
38:24	36A	85.0	85.0					Closed	Closed	.56	44,050	195,950	28.0	-2.2	13.73	94,670	67	6	3.1	0
39:50	37A	95.0	95.0					Closed	Closed	.56	46,795	208,150	28.0	-2.2	13.73	94,670	67	7	3.6	0
40:57	38A	110.0	110.0					Closed	Closed	.56	51,660	224,800	28.0	-2.2	13.73	94,670	67	8	4.1	0

REFERENCES

1. Davidson, Theron W.: Method of Net Thrust Measurement in Supersonic Flight. AGARDograph 103, Aerodynamics of Power Plant Installation, Part I, Oct. 1965, pp. 217-243.

2. Waters, Mark H.; and Graham, Philip A.: Evaluation of an Exhaust Nozzle Traversing Rake System as an In-Flight Thrust Measuring Device for an Afterburning Turbofan Engine. NAPTC-ATD-150, Naval Air Propulsion Test Center, (Trenton, N. J.), Nov. 1968.

3. Beeler, De E.; Bellman, Donald R.; and Saltzman, Edwin J.: Flight Techniques for Determining Airplane Drag at High Mach Numbers. NACA TN 3821, 1956.

4. Nugent, Jack: Lift and Drag of a Swept-Wing Fighter Airplane at Transonic and Supersonic Speeds. NASA Memo 10-1-58H, 1959.

5. Beaulieu, Warren; Campbell, Ralph, and Burcham, William.: Measurement of XB-70 Propulsion Performance Incorporating the Gas Generator Method. J. Aircraft, vol. 6, no. 4, July-August 1969, pp. 312-317.

6. Mechtly, E. A.: The International System of Units - Physical Constants and Conversion Factors. NASA SP-7012, 1964.

7. Wolowicz, Chester H.; Strutz, Larry W.; Gilyard, Glenn B.; and Matheny, Neil W.: Preliminary Flight Evaluation of the Stability and Control Derivatives and Dynamic Characteristics of the Unaugmented XB-70-1 Airplane Including Comparisons With Predictions. NASA TN D-4578, 1968.

8. Andrews, William H.: Summary of Preliminary Data Derived From the XB-70 Airplanes. NASA TM X-1240, 1966.

9. Edwards, E. L.: An Airborne Data Acquisition System for Use in Flight Testing the XB-70 Airplane. Selected Instrumentation Application Papers From AGARD Flight Mechanics Panel - Twenty-Sixth Meeting, AGARD Rep. 507, June 1965, pp. 23-48.

10. Edwards, E. L.: A Data Processing Facility for the XB-70 Flight Test Program. AGARD Conf. Proc. No. 32, 1967, pp. 243-258.

11. Ince, D. B.: Application Experience With the B-70 Flight Test Data System. Aerospace Instrumentation. Vol. 4 - Proceedings of the Fourth International Aerospace Symposium, College of Aeronautics, Cranfield, Eng., March 21-24, 1966, M. A. Perry, ed., Pergamon Press, Ltd., 1967, pp. 195-208.

12. Michaels, J. M.; Fisk, W. S.; McManus, H. L.; and Henderson, R. L.: YJ93-GE-3 Turbojet Engine. Rep. No. R61FPD321, Flight Propulsion Div., General Electric, Sept. 1961.

13. Putnam, Terrill W.; and Smith, Ronald H.: XB-70 Compressor-Noise Reduction and Propulsion-System Performance for Choked Inlet Flow. NASA TN D-5692, 1970.

14. Anon.: General Electric Company Model Specification YJ93-GE-3 Engine - Specification No. E-757 F. Flight Propulsion Div., General Electric, Feb. 9, 1959.

NASA-Langley, 1970 —— 2 H-596

"The aeronautical and space activities of the United States shall be conducted so as to contribute . . . to the expansion of human knowledge of phenomena in the atmosphere and space. The Administration shall provide for the widest practicable and appropriate dissemination of information concerning its activities and the results thereof."

—NATIONAL AERONAUTICS AND SPACE ACT OF 1958

NASA SCIENTIFIC AND TECHNICAL PUBLICATIONS

TECHNICAL REPORTS: Scientific and technical information considered important, complete, and a lasting contribution to existing knowledge.

TECHNICAL NOTES: Information less broad in scope but nevertheless of importance as a contribution to existing knowledge.

TECHNICAL MEMORANDUMS: Information receiving limited distribution because of preliminary data, security classification, or other reasons.

CONTRACTOR REPORTS: Scientific and technical information generated under a NASA contract or grant and considered an important contribution to existing knowledge.

TECHNICAL TRANSLATIONS: Information published in a foreign language considered to merit NASA distribution in English.

SPECIAL PUBLICATIONS: Information derived from or of value to NASA activities. Publications include conference proceedings, monographs, data compilations, handbooks, sourcebooks, and special bibliographies.

TECHNOLOGY UTILIZATION PUBLICATIONS: Information on technology used by NASA that may be of particular interest in commercial and other non-aerospace applications. Publications include Tech Briefs, Technology Utilization Reports and Notes, and Technology Surveys.

Details on the availability of these publications may be obtained from:

SCIENTIFIC AND TECHNICAL INFORMATION DIVISION

NATIONAL AERONAUTICS AND SPACE ADMINISTRATION

Washington, D.C. 20546